ABSTRACT

Squirrel Cage Induction Motors (SCIM) are largely prevailing machines which areused to convert electrical energy into mechanical energy in a wide number of applications in rolling mills, petrochemical industries, power plants etc.

In the thesis work, I have discussed about the major Induction motor faults like rotor faults, bearing faults, stator winding faults, air-gap eccentricity, unbalance supply fault and load faults etc. The possible causes or stresses for the occurrence of these faults are also been listed in the thesis. Wide discussion on different types of harmonics, related to these faults, is also provided in this literature. Thesis also gives a detailed literature survey in the field of data dimension (Current signals) reduction using Park's Vector approach.

Fast Fourier Transform (FFT) is a spectrum estimation technique, comprehensively used with **Motor Current Signature Analysis** (**MCSA**). However FFT does not bestow us with substantial outcome when frequency resolution is taken into account. **Multi Resolution Analysis (MRA)** is used to analyse any signal in order to obtain better resolution. **Discrete Wavelet Transform (DWT)** gives a superior idea about the variation in specific frequency band all through the bearing fault(s).

In this thesis, for fast analysis and minimalism, **Current Signal Energy** calculation is described. The different fault cases have been created using artificial signals for validation. The variation in the energy of healthy and faulty conditions gives us a fair idea relating to fault detection. Actual data analysis reveals that FFT is not suitable for practical situations. Comparative study of DWT and WPT has been done to provide a deep insight into early detection of rotor fault and bearing fault.

MATLAB based analysis has developed a "Base-Algorithm" so that it can be processed on by any non-programming personal too for further implementations in the fields like condition monitoring of SCIM in case of severefaults, provided the studies are being held on Steady State Currents.

Chapter 1

Introduction

Squirrel Cage Induction Motors are widely used mode of converting electrical energy to mechanical energy. They consume more than 60% of the electrical energy produced. These are present in major industrial applications. Hence, the maintenance of induction machines is one of the aspects where the industry most focuses its efforts, particularly since the appearance of low-cost motors in the market. Traditionally, induction motors were conceived as robust machines. However, due to the fact that low-cost motors usually work near the critical part of material characteristics, non-security margins appear and the probability of a fault increases, even more since inverters are used to drive the motor. Inverter drives introduce alterations such as dv/dt or common mode voltages that could cause premature damage to the machine, which is likely to evolve into a mechanical crash.

In a squirrel cage rotor laminated steel carries the magnetic flux and transfers heat. Also, it gives a cage like structure. Rotor bars are generally made of copper or aluminium. The squirrel cage winding carrying current will produce a torque. Shaft is provided with bearings. To cool the motor, air flow is provided by fans present on the rotor. Squirrel cage motor today includes around 80% of all industrial and commercial sectors. Within an industry, motors have different levels of reliability that can vary in size, types, and their applications.

The study of SCIM failure/fault is of great interest for researchers and plenty of algorithms of different kind have been advanced to detect it.The dominant reason of frequently occurring bearing failures are fatigue, wear, improper installation, electrical discharge, deficient lubrication, mechanical vibration, excessive temperatures, and operations at non-specified conditions.

Study of these stresses is based on current monitoring; and so it is not very expensive.Steady state data based Motor Current Signature Analysis (MCSA) is an indispensable technique, used for extracting the **current harmonics** caused by faults, in which frequency domain signal processing technique like Fast Fourier Transform (FFT),Short-Time Fourier Transform (STFT), Park's Vector Approach, Gabor Transform and Wavelet Transform are used for detection of common faults in Induction motors. FFT is easy to implement but it has a limitation that it cannot detect transient faults.

Short-Time Fourier Transform can detect transient faults but it has a drawback to detect signals in fixed window size, which results in poor frequency resolution. However, Time-scale techniques have become popular because they can overcome all the above problems using variable size window.

In this MCSA technique, current spectrum of Induction motor is used, which contains significant information of motor faults. The frequency spectrum of faulty motor is completely

different from that of healthy motor. It locates specific harmonic current component. Motor Current Signature Analysis (MCSA) are used to detect common faults in Induction motor such as rotor faults, bearing faults, stator winding faults, air-gap eccentricity fault and load faults. The above mentioned method requires continuous monitoring of motor stator current and explore for presence of various faults in Induction motor operated under constant and variable load conditions.

For understanding how the **strength (Energy)** of the fault signals is distributed in the frequency domain, the Parseval's theorem is used in a modified form. For instance, if a measured waveform is a current signal with additive disturbances due to any of the fault signals, we need to build a mechanics for categorizing the fault or suppress the frequency of the specific band. This can be done by being cognizant of energies of different bands.

1.1 Objectives of Project Work

The **Objective** of this project is to analyse the variations in **Stator Current Signal** by pursuing the **Energy** changes for different **Frequency Bands** caused by continuous variations in operating conditions due to **Variable Loadings** on 3-phase SCIM.

In order to fulfil the mentioned objective, we first reduced the sophisticated 3-phase calculations into a more informative two-dimensional data viz. **Direct (d) Axis** and **Quadrature (q) Axis** by using the **Park's Vector** approach. The first analysis is emphasized on to catch the most affected dimension due to load variations. The different components (dimensions) d and q are processed through the most recent **Signal Processing Technique** i.e. **DWT** to reduce the bulkiness of d/q- spectra. A 5-level DWT is used for this. This located only the data that comprise almost all the information related to the d/q- spectra. The approach to calculate the energy of this data is very much similar to the Spectrum Energy Calculation($E = \sum_{i=0}^{n} |Xi|^2$) of any signal.

Though, the deviation has not been a concern but the Energy, by processing the Current Signature through all above mentioned techniques without losing any information. The final approach is**Graphical** to study the various Energy Signals for different conditions. All the signatures are compared in a graphical form and dominating dimensions have been found out. Moreover, the main advantage of using DWT can be significantlyseen in the graphical viewing as the most affected part is easy to recognize, be it a **Detailed Component** or an **Approximate** one. Due to the base of bifurcation being their **Frequency Ranges**, an insight of the frequency variation can be achieved significantly showing the introduction and reduction of various frequencies that might be useful for further studies.

This **MATLAB** based analysis is further developed as a "Base- Algorithm" so that it can be processed on by any non-programming personal too for further implementations in the field like condition monitoring of SCIM in case of sever **Faults** provided the studies are being held on **Study State** Currents.

1.2 Orientation

The project work explores the frequency bands affected due to harmonic after occurring of faults. The different operating conditions are depicted as Energy bar graphs and the whole process is compiled in this report as mentioned:

Chapter 1 presents an overview of the work by providing a brief of various conditions and techniques included in work with an organized orientation.

Chapter 2 provides a brief literature on Induction Motor. The various operating conditions, different faults and their relation with fundamental frequencies with formulas is also shown in this chapter.

Chapter 3 describes the need of condition monitoring by providing a brief of fault diagnosis. It also presents a view of various available techniques for the condition monitoring purpose.

Chapter 4 discusses the Wavelet Transform as a novel approach for our work. It provides a deep insight of various signals and justifies the edge of DWT over other techniques like FFT while working in time-frequency domain. Filtration chart of DWT is also presented in the chapter. An overview of Parseval's theorem is also provided.

Chapter 5 is a transitory overview of the validation by use of artificial signals that are representatives of different working conditions.

Chapter 6 embarks upon the significance of energy changes in various frequency bands in case of bearing faults and rotor cut faults. Depiction of all energy-bar-plots is concluded with a discussion over the results.

The references are mentioned at the end of the report.

Chapter 2

Common Faults in Induction Motor

2.1 Introduction

Nowadays a variety of industrial applicationsthree-phase make use of Squirrel Cage Induction Motors (SCIMs) due to their ruggedness, cheapness and requirement of low maintenance. The motor lifetime can be reduced considerably due to the voltage stresses caused by the modern high frequency power converters in addition to corrosive and dusty industrial environments where these motors are installedfor operation.

2.2 Induction Motor - Overview

Induction Motors are most widely used electro-mechanical device which converts electrical energy into mechanical energy via electromagnetic induction in industries as they are robust, cheap efficient and reliable. Also it requires less maintenance and sufficiently high starting torque.

2.2.1 Squirrel Cage Induction Motor (SCIM)

Generally, Induction motors are used in pumps, machine tools, conveyors, presses, elevators, centrifugal machines, packaging equipment etc. Other applications are in petro-chemical and natural gas plants, equipment for coal plants, shredders etc. Therefore, it becomes very important to run them smoothly so that production can be maintained. An Induction machine is an asynchronous machine which contains a magnetic circuit that links with two electric circuits and rotates with respect to each other and the power is transferred from one electrical circuit to other. The rotor winding in three-phase induction motor can be squirrel cage type or wound-rotor type.

On the basis of rotor winding Induction motors can be classified under following two categories:

- Squirrel Cage Induction Motor
- Wound Rotor Induction Motor

Out of the two above mentioned types, squirrel cage Induction motors are most often used as they are simpler, more rugged and are more efficient than slip-ring Induction motors. The squirrel cage Induction motors are preferred because they are low on cost, have no brushes and commutators and are more suitable for high speed applications[10], [11].

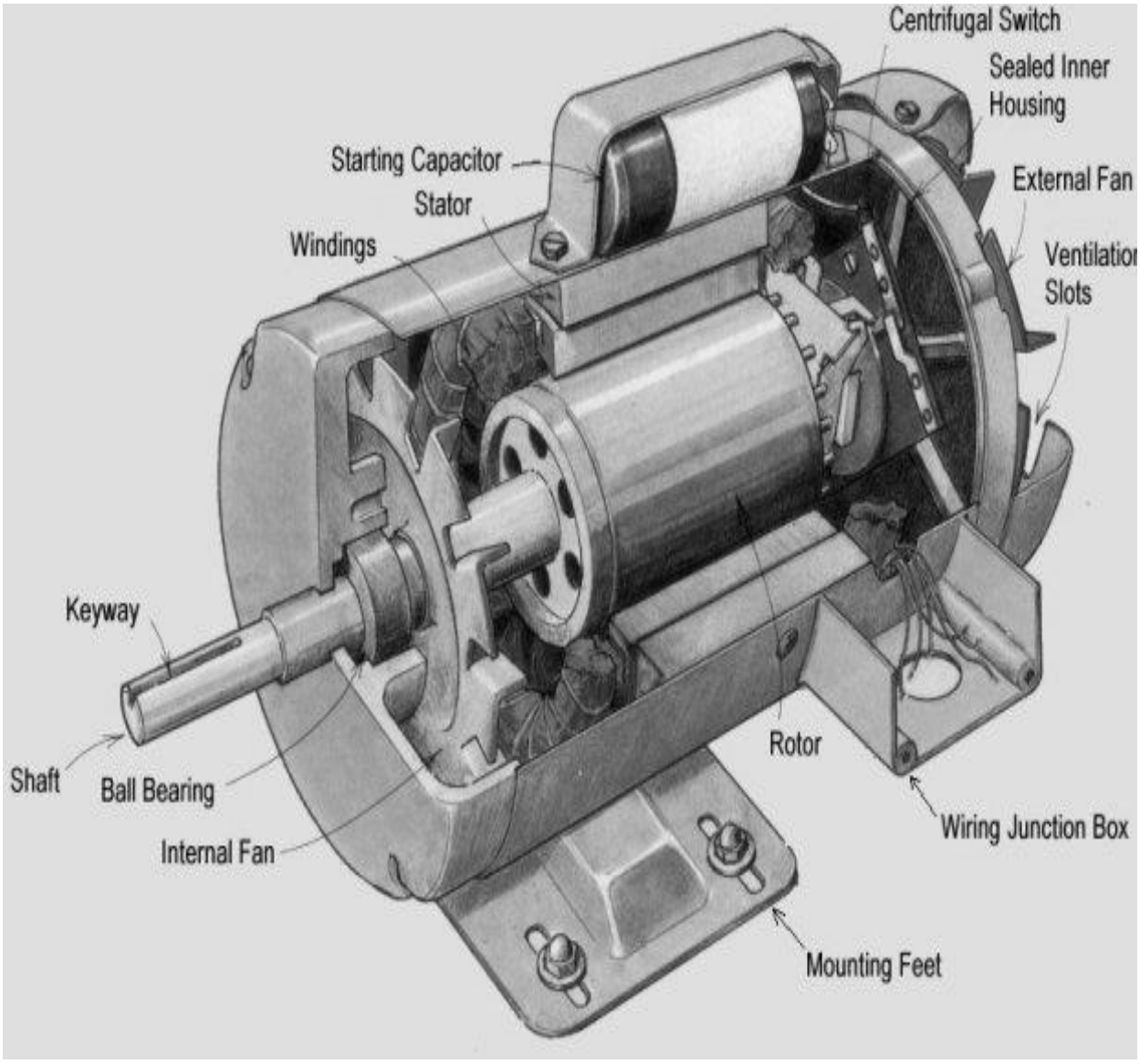

Fig. 2.1. View of an Induction motor (Source: www.sawmill.creek.org)

Around 90% of Induction motors are of squirrel cage type, because of their simple and rugged construction. The rotor contains a cylindrical laminated core with parallel slots carrying rotor conductors which are shorted at each end by end-rings. Rotor bars are generally made of copper, aluminum or alloys. The end-rings and conductors form a cage like structure which was earlier used for keeping squirrel, thus the name squirrel cage rotor. The rotor bars are slightly skewed to provide uniform torque, reduce noise during operation and also to reduce locking capacity of the rotor [2], [3].

The common faults that occur in induction motors are: bearing faults, rotor faults, short turn winding fault, gear fault and misalignment of shaft. The internal faults in induction motors are classified as:

- Electrical Faults
- Mechanical Faults

Electrical faults [30], [31] are either caused by winding insulation problems or due to rotor faults and include rotor faults and short turn faults. While mechanical faults [32] contains air-gap eccentricity, bearing faults, load faults and misalignment of shaft.

2.3 Electrical Faults

2.3.1 Broken Rotor Bar/ End-rings:

A squirrel cage induction motor contains rotor bars and end rings. Due to frequent start or manufacturing defect or thermal stresses a rotor bar may be completely broken or partially cracked. As per the survey, these causes around 5-10% faults in induction motor. This broken rotor bar condition causes sideband components to appear. These sideband components are found on the left and right sides of the fundamental frequency component when seen in the power spectrum of the stator current. The left sideband component are found due to electric and magnetic asymmetries in the induction motor rotor cage, while the right sideband components occur due to speed ripples caused by the torque pulsations [45]-[51]. The frequencies of this sideband can be given as [1], [5]-[9]:

$$f_{sb} = (1 \pm 2s) f_s \qquad (1)$$

The frequencies of broken rotor bar/end-rings are given as [1], [5], [7]:

$$f_{bb} = f_s \left[k\left(\frac{1-s}{p} \right) \pm s \right] \qquad (2)$$

where, k/p = 1,5,7,11,13,….(because of normal winding configuration),

s = per unit slip, f_s = fundamental frequency of stator current (supply).

The rotor fault produces a series of sideband frequencies given as [12], [13]:

$$f_{sb} = \left(1 \pm n2s\right) f_s \qquad (3)$$

where, n = 1, 2, 3 … = order of harmonics.

The broken rotor bar and end ring breakages also throw a light on torque ripples, speed oscillations, stator current envelope and instantaneous stator power oscillations.

2.3.2 Stator Winding Fault:

These causes around 35-40% induction motor failures. These fault results generally due to long-term thermal aging. These are usually caused by insulation failure in various turns of a stator coil. Due to stator turn fault in three phase induction motor a large circulating current is produced and consequently an excessive heat in the shorted turns is generated. If motor is operated above its temperature limit, the best insulation may fail easily. The life of insulation decreases by 50% for

every 10º C rise in the stator temperature limit.Thus, efficient detection of stator insulation failure is crucial for harmful motor failure [52], [53].

The major causes of winding insulation failures are [13]:

- Short circuit
- High winding temperature
- Loose bracing on end winding
- Contamination due to oil, dirt and moisture
- Electrical discharges
- Leakage in cooling system

The stator winding related failures are categorized into five main parts shown in Fig. 2.2:

a) Turn-To-Turn
b) Coil-To-Coil
c) Line-To-Line
d) Line-To-Ground
e) Open-Circuit Fault

Out of all the above mentioned faults, turn-to-turn faults are most difficult one to detect. Further these faults are very challenging to detect at their initial stages, still various condition monitoring techniques are used to detect them.

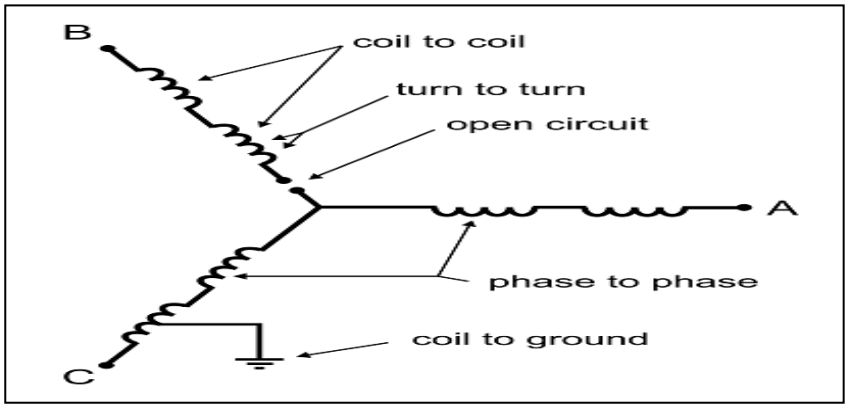

Figure (2.2). Different types of short winding faults

2.4 Mechanical Faults

The commonly found mechanical faults in three phase induction motors are:

2.4.1 Bearing Faults:

These faults account for around 40% of all induction motor failures. Bearings are very common component of electrical machines. These are employed to support motor shaft. These consist of inner and outer rings. The main cause of bearing failure is improper installation of bearing or shafts. Corrosion and contamination also causes bearing failure in most of the industries. The most common reasons for bearing failures can be listed as follows [54]:

- Vibrations
- Thermal Overloading
- Shaft misalignment
- Excessive overloading
- Defects in machinery
- Improper handling
- Damaged during storage or transportation

Due to abnormal running of bearing, large vibrations are produced and noise level is also increased. If any of the thermal, mechanical or magnetic stresses exceeds the bearing capacity, then, the bearing may get damaged and a catastrophic failure can occur. Exceeding the limiting speed and overload can also be the possible causes of bearing failure. Causes may include improper lubrication of bearings, improper maintenance and storage. Increased noise level or vibration level are the general indications of bearing failure [18], [23], [24], [55]-[56].

The mechanical displacement in ball bearing due to the damaged bearing causes a change in machine air-gap. The characteristic frequency of ball bearing is related to ball-bearing dimension (fig. 2.3), rotational frequency of the machine. These variations produce stator current at frequencies [1], [5], [7]-[9]:

$$f_b = f_s \pm n f_{i,o} \quad (4)$$

$$f_{i,o} = \frac{n}{2} f_r \left[1 \pm \frac{BD}{PD} \cos\beta \right] \quad (5)$$

where, n_b = number of balls, f_r = rotational frequency in RPM,

PD = bearing pitch diameter,

BD = ball diameter,

β = contact angle of ball with the races.

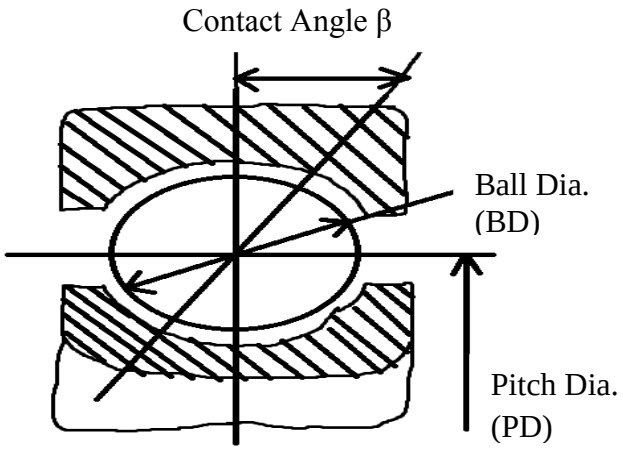

Figure (2.3): Ball-bearing dimension

2.4.2 Air-gap Eccentricity:

Air-gap eccentricity is very common fault in induction motor and this occurs due to the unequal air-gap between stator and rotor [57]-[59]. This fault generates problems of vibration and noise. These may lead to unequal magnetic pull (UMP) and subsequently can cause a stator to rotor rub which may lead to stator or rotor damage. UMP is the situation raised due to the non-uniform air-gap between stator and rotor through deformations or manufacturing tolerances.

It also causes the rotor bending and striking to the stator winding. For an ideal case, the rotor is centrally placed in the air-gap and the balanced magnetic forces are in opposite direction, with no rotor deflection [60]. The main causes of air-gap eccentricity are: inaccurate positioning of rotor with respect to stator, shaft deflection, bearing damage and stator core movement.

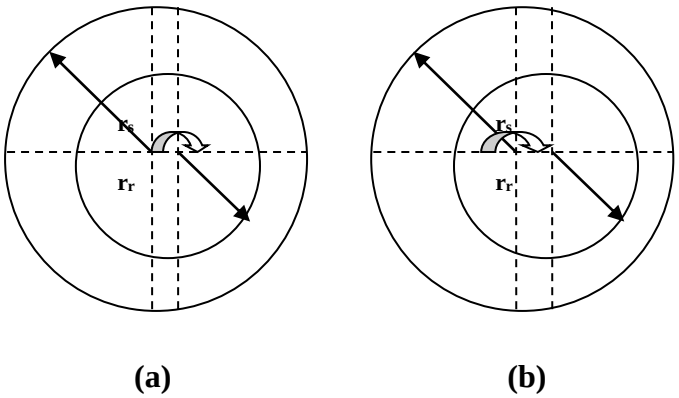

Figure (2.4): (a) Static eccentricity and (b) Dynamic eccentricity

There are following types of air-gap eccentricity:

a) Static Eccentricity

b) Dynamic Eccentricity
c) Mixed Eccentricity

Static eccentricity means the condition of inaccurately placed motor shaft in the air-gap shown in Fig. 2.4 (a). Its main cause is incorrectly installed rotor or oval stator core.

Dynamic eccentricity means centre of rotation and centre of rotor do not coincide with each other shown in Fig. 2.4 (b). It is caused due to bearing wear, misalignment of bearing or shaft.

Static eccentricity is space dependent while dynamic eccentricity is space and time dependent. The combined static and dynamic eccentricity is known as mixed eccentricity. The air-gap eccentricity up to 10% is usually allowed, however, it is kept low to avoid vibration, noise and UMPF. Air-gap eccentricities occur even in newly manufactured motors. These eccentricities can be detected by two methods.

1. The sideband frequencies linked due to eccentricities are given as [28]:

$$f_{slot+ecc} = f_s\left[\left(kR \pm n_d\right)\left(\frac{1-s}{p}\right) \pm n_w\right] \qquad (6)$$

2. The abnormal harmonic frequencies due to both static and dynamic eccentricities are given by [7]:

$$f_{ecc} = f_s\left[1 \pm m\left(\frac{1-s}{p}\right)\right] \qquad (7)$$

where, f_s = supply frequency, k = 1, 2, 3…,R = rotor slot number; n_d = eccentricity order;

s = per-unit slip; p = no. of pole pairs; n_w = stator mmf harmonics order.

m = 1, 2, 3…

2.4.3 Load Faults:

If the load toque is not changing with rotor position, then current will have some spectral components which are similar to those arise due to fault condition. Motors are very commonly coupled to mechanical loads and gears in industries. Several faulty conditions may occur in this arrangement. Examples can be given by faulty gear system or coupling misalignment which couples a load to the motor [5], [7], [11].

2.4.4 Motor Shaft Failure:

Majority of shaft failures occurs due to the combination of various stresses. Motor shaft is generally made of hot rolled carbon steel or alloyed steel. Major possible causes of shaft failures also include corrosion, brittle fracture, and fatigue or overload [61]. 80-90% shaft failures are fatigue related.

Common causes of shaft failures are listed in Table 2.1 below:

Table 2.1 Causes of Shaft Failures.

Failures	Causes
Corrosion	wear pitting or cavitation
Fatigue	excessive rotary bending
Overload	quick stop or jam

Chapter 3

Discussion of Various Existing Techniques

3.1 Introduction

This chapter includes, literature survey on condition monitoring techniques in Induction motors. This survey covers some important topics such as need for condition monitoring techniques, fault diagnosis and existing condition monitoring techniques.

3.2 Need for Condition Monitoring

Condition monitoring techniques have been defined as the continuous observation of the health of a plant and equipment throughout its entire service life. It is very crucial to detect faults in nascent conditions to provide a safe environment in plants and industries. These condition monitoring techniques give early warning of motor failure.

As a result, we can easily plan what preventive measures to be taken in future and when to do the repair work. Consequently, outage time and down time is reduced. Therefore, by using effective condition monitoring techniques, we can improve reliability, productivity and safety of the system [11].

All of the present conditions monitoring techniques require the operator to have deep knowledge so that one can easily make the difference between the healthy and faulty motor conditions. Many condition monitoring techniques have been proposed to diagnose faults in electrical machines. Many large machine systems are coupled with mechanical or vibration sensors. But these are very expensive and delicate.

In many cases, vibration monitoring methods are used to diagnose faults. But it is advisable to go for stator current monitoring technique since it can provide the same result as in vibration monitoring but in non-invasive manner. This technique utilizes stator current data to detect fault. Sometimes transient time current data is also used for the fault detection.

The parameters chosen for condition monitoring should be such that it will provide the complete information to the operator and maintainer for plant maintenance. Apart from traditional monitoring techniques like line currents, voltages, thermal and vibration monitoring, quantities like rotational speed and leakage fluxes are also being recently used for monitoring.

3.3 Fault Diagnosis

The study of induction motor behaviour and their diagnosis always has been a very challenging task for electrical engineers and researchers. Induction motors are prone to many types of faults. If a fault is not detected in its initial stage then it may become severe and induction motor may suffer from permanent damage. Thus, undetected motor fault cause motor failure, which in turn result into production shutdowns.

The term fault diagnosis means to determine a particular fault in the system. The fault diagnosis process usually consists of four phases, as shown in Fig. 3.1. Fault diagnosis will provide following advantages to the system:

- Predict system failure.
- Reduced maintenance cost.
- Improved reliability.
- Improved equipment performance.

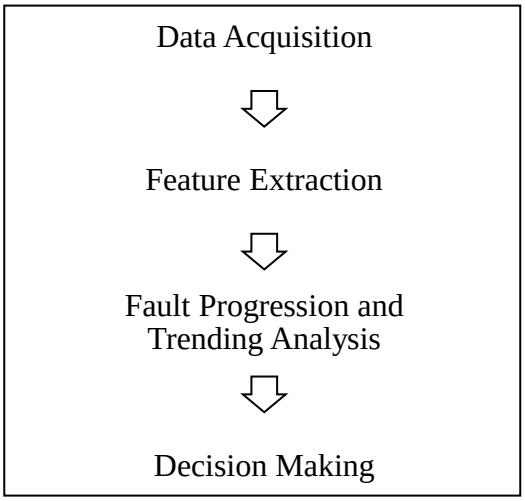

Figure (3.1): Fault Diagnosis Process

1. Data Acquisition:

This is the method of converting real-time signals into some numeric value so that computer can understand it [15]. Basically, data acquisition is a method to convert analog signals or waveforms into digital signals or values. The data acquisition system mainly consists of following components:

- **Sensors-** These convert physical quantities into electrical signal.
- **Signal Conditioning Circuitry-** It converts electrical signals into a form that can reliably be converted to data of relevance.
- **Analog to digital converter-** These convert conditioned electrical signals to some numerical values.

Thus, the data acquisition system starts with the measurement of physical properties like voltage, current, temperature, gas pressure etc. Before measuring these quantities, they must be first converted into a form which can be sampled by the data acquisition system.

Therefore, sensors, here, acts as transducers, which convert a physical phenomenon into a corresponding electrical signal (e.g. strain gauge). Signal conditioning is required if the signals from the sensors are not suited to the data acquisition system hardware used. Then, the filtering or amplification of signal is required. Finally, these signals are converted to digital form and can be encoded to reduce transmission errors.

2. Feature extraction:

It is mainly a type of reduction in dimensions. If the input data to an algorithm is very large to be processed then, the input data is converted into a reduced set of significant data. Converting input data into the set of significant data is called Feature extraction. If the features

extracted are suitably chosen then, it is expected to represent all relevant data in reduced form instead of taking full input data [14], [15].

3. Fault progression and Trending analysis:

Fault progression is the deep observation of fault, how it develops and how it progresses with time. These features tell the behaviour of fault. Trending analysis is the analysis or observation of a system to develop a pattern or trend, in the observed data. It is generally used to predict future events.

4. Decision making:

This is the method of selection of an action which is based on outcomes of above mentioned procedures. This can be done by some classical or artificial intelligence techniques like expert system, fuzzy controller etc.

3.4 Existing Condition Monitoring Techniques

In recent years, many techniques [5]-[9] have been developed for detecting and monitoring above mentioned faults in Induction motors and these can be categorized as:

- Thermal Monitoring
- Torque Monitoring
- Noise Monitoring
- Vibration Monitoring
- Electrical Monitoring-
    - ❖ **Motor Current Signature Analysis**
        i. Fast Fourier Analysis
        ii. Current Park's Vector Approach
        iii. Wavelet Transform Analysis

3.4.1 Thermal Monitoring:

Thermal Monitoring in induction motor is completed by temperature measurement method or by the parameter estimation method. This method is an indirect method of motor fault detection. This method can be used to detect some of the stator faults like turn-to-turn and bearing faults. For a turn-to-turn fault, the temperature rise in the fault region is too slow to detect faults unless it becomes a more severe fault like phase-to-phase or phase-to-neutral fault. In the shorted turns of stator current fault, a large amount of heat is produced locally; and this heat proves the intensity of fault [17].

3.4.2 Torque Monitoring:

In all induction motor faults, sidebands are produced around the characteristic frequency within air-gap torque. This air-gap torque cannot be measured directly. The instantaneous

power does not truly represent the instantaneous torque. A torsional spring system is accomplished by the output terminals, the shaft, the rotor and the mechanical load which has its own frequency.

3.4.3 Noise Monitoring:

By analysing the acoustic noise spectrum, noise monitoring is accomplished. For fault detection, acoustic noise from air-gap eccentricity can be used. This method of monitoring is not very accurate since measurement of noise due to air-gap eccentricity becomes difficult due to the noise coming from other machines.

3.4.4 Vibration Monitoring:

All electric motors produce noise & vibration & these can be used to find the condition of the motor. Forces of magnetic, mechanical and aerodynamic origin are the causes of noise and vibrations in electrical machines. The radial forces produced due to the air-gap field are the major causes of vibration & noise production in electrical motors. Vibration monitoring is the best condition monitoring technique but it requires costly accelerometers. Thus, cost is the major disadvantage in using vibration monitoring. Bearing faults, air-gap eccentricity and rotor asymmetry are usually detected using this method. Vibration monitoring is non-intrusive, continuous and convenient process of monitoring [18]-[21].

3.4.5 Electrical Monitoring:

Some techniques like Current Park's vector approach, Current signature analysis, Fast Fourier Transform, Wavelet analysis all fall under this category. In this method, generally stator current is used to detect various motor faults. Thus, it is a non-intrusive current monitoring technique which does not require any extra equipment [18]-[20], [22]-[24].

3.5 Motor Current Signature Analysis

MCSA technique has been used in numerous applications like nuclear generation, industries etc. Out of above mentioned techniques, MCSA is the best technique [4], [5], [7], [16], [25]-[27], known till date since it does not require any additional device/ instrument, are not very expensive, easy to implement and also non-intrusive.

A. Fast Fourier Analysis

A Fourier Transform converts time-domain content to frequency-domain. A Fast Fourier Transform (FFT) is an algorithm to calculate the Discrete Fourier Transform (DFT) and its inverse. FFT is a very fast computation method and used in large calculation of engineering and mathematics [5], [7], [16], [26], [28], [29].

B. Current Park's Vector Approach

Next electrical monitoring technique is current Park's vector approach [5], [7], [16], [30]-[33]. In general, a two-dimensional representation can be used to describe three-phase Induction

motor phenomenon, using Park's Vector. The main phase variables (i_a, i_b, i_c) can be represented as Park's vector components (i_d, i_q) as:

$$i_d = \sqrt{\frac{2}{3}} i_a - \frac{1}{\sqrt{6}} i_b - \frac{1}{\sqrt{6}} i_c \qquad (8)$$

$$i_q = \frac{1}{\sqrt{2}} i_b - \frac{1}{\sqrt{2}} i_c \qquad (9)$$

Under ideal conditions, the three-phase current results into following Park's vector component:

$$i_d = \frac{\sqrt{6}}{2} i_m \sin \omega t \qquad (10)$$

$$i_q = \frac{\sqrt{6}}{2} i_m \sin\left(\omega t - \frac{\pi}{2}\right) \qquad (11)$$

Where, i_m = maximum value of supply phase current;

ω = supply frequency;

t = time variable.

For an ideal case, it is represented as a circular pattern centred at the origin of co-ordinates shown in Fig. (**3.2**). Abnormal condition is detected by monitoring the deviations from the acquired pattern.

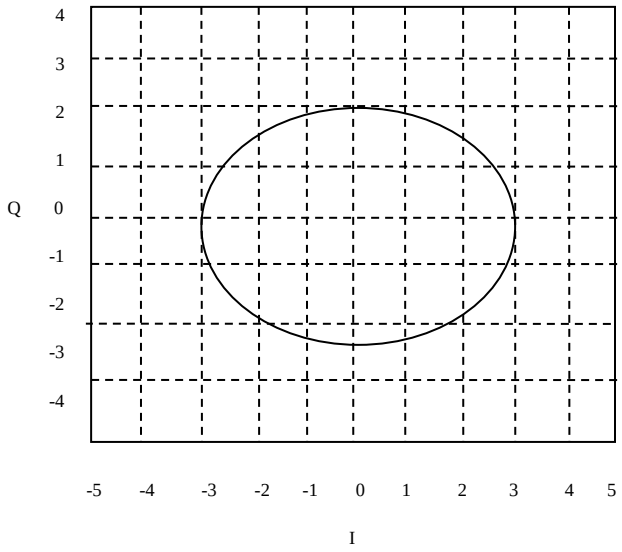

Figure (3.2): Current Park's Vector for Ideal Condition

C. Wavelet Analysis

Wavelet analysis is fast, more accurate, more convenient & highly sensitive for on-line detection of fault. This method is based on the idea of reconstruction of signal from some significant set of signals of variable amplitude fixed shape. This method can be used to detect any type of fault under any load condition [34]-[44], [62]. The explanatory details are provided in next chapter.

Chapter 4

The Wavelet Transform

4.1 Introduction

The Wavelet Transform (WT) is a transform of the typethat provides the time-frequency representation together. Many times a particular spectral component occurring at any instant can be of particular interest. In these cases it may be very beneficial to know the time intervals, these particular spectral components occur.

For example, in EEGs (electroencephalogram), the latency of an event-related potential is of particular interest (Event-related potential is the response of the brain to a specific stimulus like flash-light, the latency of this response is the amount of time elapsed between the onset of the stimulus and the response).

Fourier techniques have been the mainfrequency-domain analysis tool in many applications ofdigital relays. However, the signals generated by the powersystem faults and processed by these relays are rich inelectromagnetic transients. Thus, one of the main problems with these techniques or other similar ones is the width of thewindow function used as these signals are non-stationary. However, in a non-stationary signal there exists atransition period in which the moving data window containsboth pre-fault and post-fault samples. The ensuring Fourier transform results are unreliable.

To overcome these problems the WT has been consideredas an alternative to the Fourier techniques. It is a linearoperation that decomposes a signal into several other signalsof different scales with different time and frequencyresolutions. These are resulting from the simultaneousperformance of two operations (scaling and translation) on asingle “window” function, called “mother wavelet”. This is acompact support and oscillatory function with zero averageand quick deadening at both ends.

4.2 Characteristics of Wavelet Systems

- Basis functions are generated from a single wavelet or scaling function by scaling and translation.
- Exhibit multi resolution characteristics viz. dilating the scaling functions provides a higher resolution space that includes the original signal.
- Lower resolution coefficients can be computed from higher resolution coefficients through a filter bank structure.

4.2.1 Reasons for Selecting Wavelet Transform:

- Provide unconditional basis for large signal class.Wavelet coefficients drop-off rapidly thus, good for compression, de-noising, detection/recognition which is the goal of any expansion.
- Having the coefficients which provide more information about signal than time-domain.
- Having most of the coefficients be very small (sparserepresentation) while Fourier Transform (FT) is not sparse for transients.
- Accurate local description and separation of signal characteristics.Fourier puts localization information in the phase in a complicated way whereas Short Time Fourier Transform (STFT) can't give localization and orthogonality.
- Computation of wavelet coefficient is well-suited to computer becauseno derivatives of integrals needed and turns out to be a digital filter bank.

The wavelet transform, an extension of the Fourier transform, projects the original signal down onto wavelet basis functions and provides a mapping from the time domain to the timescale plane. The wavelet basis functions are localized in the time and frequency domain. They are obtained from a single prototype wavelet, the "mother" wavelet, through the process of dilation and translation. Using scaling and translation operations to the mother wavelet, a family of wavelet functions is created with the same shape as the mother wavelet but of differentsizes andlocation.

The common families of wavelets are:

- Wavelets for Continuous Wavelet Transform (Gaussian, Morlet etc.)
- Symlets
- Coiflets
- DaubechiesMaxfelt Wavelets
- Biorthogonal Spline Wavelets
- Complex Wavelets

4.3 Multi Resolution Analysis (MRA)

MRA, as implied by its name, analyzes the signal at different frequencies with different resolutions.MRA is designed to give good time resolution and poor frequency resolution at high frequencies and good frequency resolution and poor time resolution at low frequencies. This approach makes sense especially when the signal at hand has high frequency components for short durations and low frequency components for long durations. Fortunately, the signals that are encountered in practical applications are often of this type.

Wavelet transform gives both time-frequency and time-scale analysis with multi-resolution characteristics. Due to these reasons, they are much efficient in fault diagnosis in Induction motors under variable load conditions.The WT has a good time and poor frequency resolution at high frequencies, and good frequency and poor time resolution at low frequencies: In Figure 4.1, lower scales (higher frequencies) have better scale resolution(narrower in scale, which

means that it is less ambiguous what the exact value of the scale) which correspond to poorer frequency resolution .

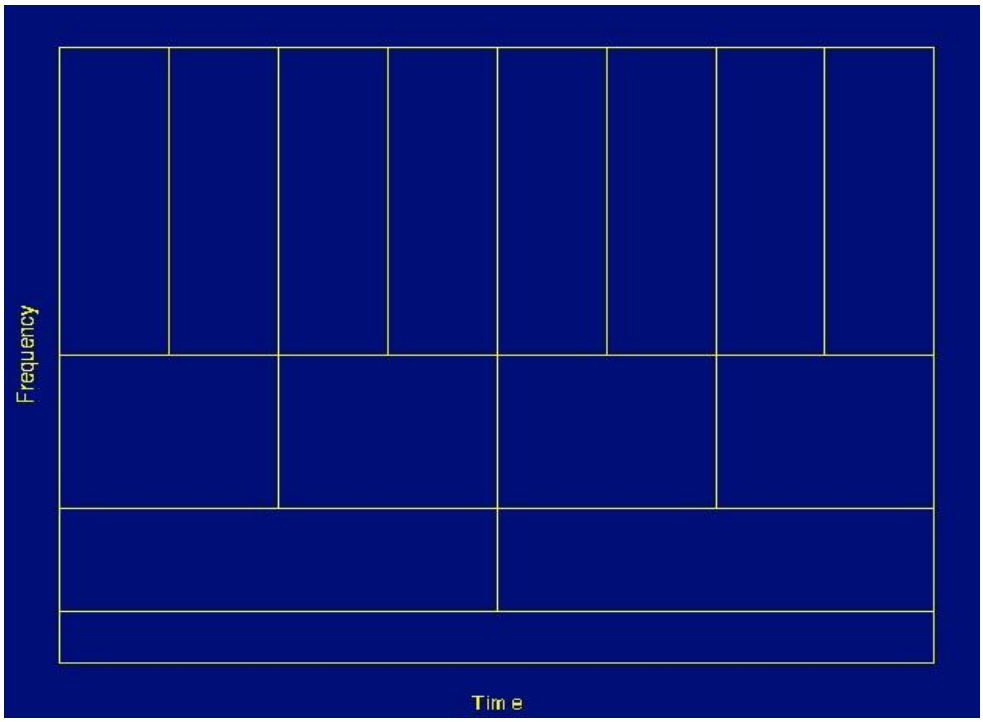

Figure (4.1): Description of MRA

Similarly, higher scales have scale frequency resolution (wider support in scale, which means it is more ambitious what the exact value of the scale is) , which correspond to better frequency resolution of lower frequencies.For the analysis purpose two types of wavelet transform can be used:

- Continuous Wavelet Transform (CWT)
- Discrete Wavelet Transform (DWT)

4.4 Continuous Wavelet Transform (CWT)

Here, for different parts of the time-domain signal, the transform is calculated separately. The CWT can be given as:

$$CWT_x^{w(t)}(t, f) = \psi_x^{\psi}(\tau, s) = \frac{1}{\sqrt{|s|}} \int x(t)\psi^* \left(\frac{t-\tau}{s} \right) dt \qquad (12)$$

Where, τ = translation parameter; s = scale parameter;Ψ (t) = transforming function (Mother Wavelet).

For CWT the parameters vary in a continuous fashion. This representation offers the maximum freedom in the choice of the analysis wavelet. From an intuitive point of view, the CWT consists of calculating a "resemblance index" between the signal and the wavelet (recall the definition of autocorrelation function.

4.5 Discrete Wavelet Transform (DWT)

As all microprocessor systems do calculations in discrete domain we need a discrete version of wavelet transform also.In Discrete Wavelet Transform (DWT), to divide the signal into a coarse approximation and detail signal, the analysis of signal is done at different frequency bands with different resolutions using digital filtering techniques. The signal is passed through low pass and high pass filters. Low frequencies are analysed by low pass filters and high frequencies are analysed by high pass filter. Two functions, Scaling function and Wavelet function associate DWT with low pass and high pass filters.

At the first stage, an original signal is divided into two halves of the frequency bandwidth, and sent to both the HPF and LPF. Then the output of the LPF is further cut into half of the frequency bandwidth, and sent to the second stage; this procedure is repeated until the signal is decomposed to a pre-defined level. If the original signal is being sampled at *fs*Hz, the highest frequency that the signal could contain, from Nyquist's theorem, would be *fs/2* Hz.

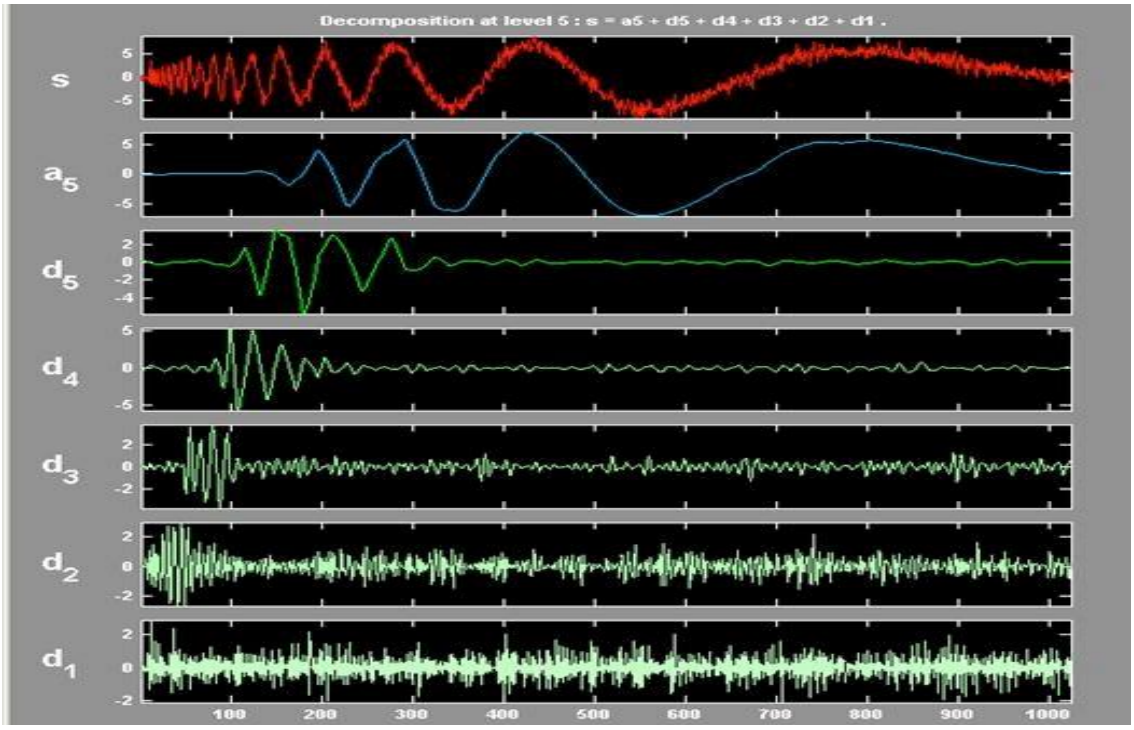

Figure (4.2): DWT Coefficients Representation

This frequency would be seen at the output of the high frequency filter, which is the first detail. Thus, the band of frequencies between *fs/2* and *fs/4* would be captured in detail 1; similarly, the band of frequencies between fs/4 and fs/8 would be captured in detail 2, and so on.

For the enhanced investigation of the fault signature, wavelet based techniques were developed. Wavelet transform becomes inevitable among the modern techniques due to the fact that it gives multi-resolution by using scaling, superior logarithmic frequency coverage. It uses a single 'window' function known as 'mother wavelet'. For decomposing the signal the execution of decomposition is done through filtering and down sampling.

The resolution of the signal, which is a measure of the amount of detail information in the signal, is changed by the filtering operations, and the scale is changed by upsampling and downsampling (subsampling) operations. Subsampling a signal corresponds to reducing the sampling rate, or removing some of the samples of the signal. For example, subsampling by two refers to dropping every other sample of the signal. Subsampling by a factor *n* reduces the number of samples in the signal *n* times.

The procedure starts with passing this signal (sequence) through a half band digital low-pass filter with impulse response h[n]. Filtering a signal corresponds to the mathematical operation of convolution of the signal with the impulse response of the filter. The convolution operation in discrete time is defined as follows:

$$x[n] * h[n] = \sum_{k=-\infty}^{\infty} x[n].\, h[n-k] \tag{13}$$

Here h[n] can be low-pass and high-pass filter's impulse response.

A half band low-pass filter removes all frequencies that are above half of the highest frequency in the signal. For example, if a signal has a maximum of 1000 Hz component, then half band low-pass filtering removes all the frequencies above 500 Hz. Half the samples can be discarded without any loss of information by down sampling the output by two.

This is possible only due to the fact that one DWT coefficient contains information of other three previous or next data also depending upon the type of filter. In summary, the low-pass filtering halves the resolution, but leaves the scale unchanged. The signal is then subsampled by two since half of the number of samples is redundant. This doubles the scale.
This procedure can mathematically be expressed as

$$y[n] = \sum_{k=-\infty}^{\infty} h[k].\, x[2n-k] \tag{14}$$

The approximate and detailed components can be mathematically expressed as follows

$$y_{high}[k] = \sum_{n} x[n].\, g[2k - n] \tag{15}$$

$$y_{low}[k] = \sum_{n} x[n].\, h[2k - n] \tag{16}$$

Where$y_{high}[k]$and $y_{low}[k]$are the outputs of the highpass and lowpass filters, respectively, after subsampling by 2.here $y_{high}[k]$ termed as detailed components and $y_{low}[k]$as approximate components.

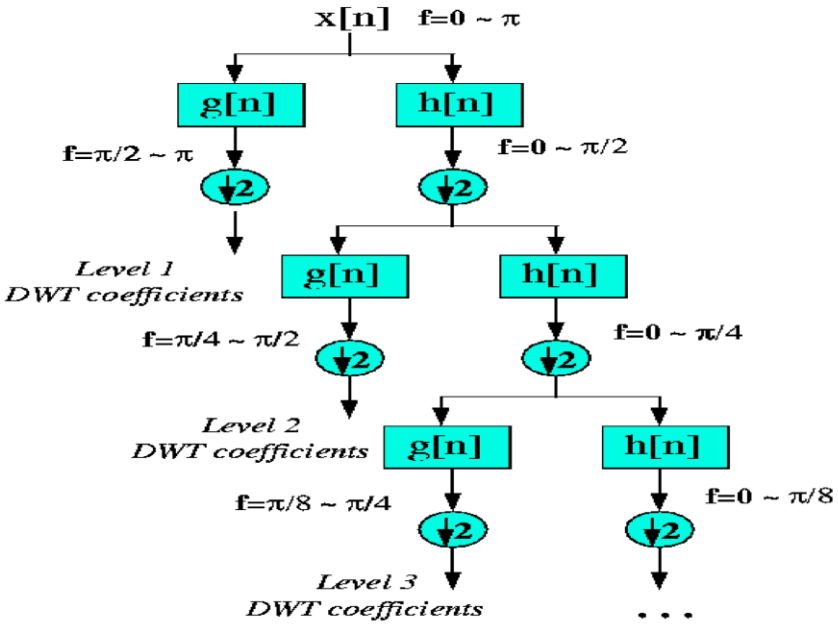

Figure (4.3) Representation of DWT

The frequencies that are most prominent in the original signal will appear as high amplitudes in that region of the DWT signal that includes those particular frequencies. The difference of this transform from the Fourier transform is that the time localization of these frequencies will not be lost. However, the time localization will have a resolution that depends on which level they appear. If the main information of the signal lies in the high frequencies, as happens most often, the time localization of these frequencies will be more precise, since they are characterized by more number of samples. If the main information lies only at very low frequencies, the time localization will not be very precise, since few samples are used to express signal at these frequencies. This procedure in effect offers a good time resolution at high frequencies, and good frequency resolution at low frequencies. Most practical signals encountered are of this type.

4.6 Wavelet Packet Transform

Wavelet Packet Transform (WPT) is an enhanced form of wavelet transform which decomposes the signal to full level. It consents to the property of orthogonality and time frequency localization. The signal is down sampled and decomposed for increased time-frequency resolution. Selection of the right frequency band based on the signal features for consistent spectrum is done by WPT. The refinement of high frequency component is the main essence of WPT as it decomposes high frequency also and improves localization.

The formulas of decomposition for DWT and WPT remain same-

$$A[n] = \sum X[n].g[2k-1] \tag{17}$$

$$D[n] = \sum X[n].h[2k-1] \tag{18}$$

Here, $A[n]$ and $D[n]$ are approximate and detailed coefficients respectively. The approximate components are further decomposed up to a certain level in case of DWT while in WPT both approximate and detailed components are decomposed for the defined level and consequently impart the better frequency resolution.

Wavelet Packet decomposes both low and high frequency components up to certain decomposition level with same length of frequency band. By n level decomposition we obtain 2^n Wavelet package coefficient vectors.

4.7 Parseval's Theorem

According to Parseval's theorem, the energy of the signal is related to the energy in each of the expansion components and their wavelet coefficients. It means that the energy of the signal can be separated according the following expansions.

$$\int |\mathrm{f(t)}|^2 \,\mathrm{d(t)} = \sum_{\mathrm{k}} |\mathrm{a(k)}|^2 + \sum_{\mathrm{j=0}}^{\mathrm{j-1}} \sum_{\mathrm{k}} \left|\mathrm{d_j}\right|^2 \tag{19}$$

Therefore the energy of signal is defined by wavelet coefficient as formula

$$\mathrm{E_{signal}} = \mathrm{E_{a_0}} + \sum_{\mathrm{j=0}}^{\mathrm{j-1}} \mathrm{E_{d_j}} \tag{20}$$

$$E_{a_o} = \sum_{k} |a(k)|^2 \tag{21}$$

$$E_{d_j} = \sum_{k} |d(k)|^2 \tag{22}$$

whereE_{a_o} is the energy of the approximated version of the decomposed signal and $E_{d_j}$is the energy at the detail version. The energy distribution features of the detailed version from distorted signal will be utilized to extract the features of power disturbances. Therefore, the detailed energy will be calculated at each decomposition level to extract the feature curve. By using Parseval's theorem, the number of transient signal features can be reduced without losing its fidelity

Chapter 5

Proposed Algorithm and Validation

5.1 Introduction

The energy is calculated for both pre fault (E_h) and post fault (E_f) conditions. The percentage deviation in energy content of faulty signal vis-a-vis healthy one is treated as fault signature (FS).

$$\%FS = \frac{E_f - E_h}{E_h} \times 100 \quad (23)$$

A Fault Signature (FS) vector based on signal energy vector can be formed, which is then used for performing bearing fault analysis. This %FS can be used as a direct parameter of the fault content as it does not contain the signal energy of healthy time.

Table 5.1 Artificial Signals for Validation

Motor Condition	Signal
Healthy	Sin(2πft)+(0.3)Sin(6πft)+(0.2)Sin(10πft)
Faulty Case I	Sin(2πft)+(0.31)Sin(6πft)+(0.19)Sin(10πft)
Faulty Case II	Sin(2πft)+(0.3)Sin(6πft)+(0.2)Sin(10πft)+(0.05)Sin(14πft)
Faulty Case III	Sin(2πft)+(0.3)Sin(6πft)+(0.2)Sin(10πft)+(0.05)Sin(14πft)+(0.02) Sin(18πft)

f=50 Hz (Let)

The healthy current signal energy serves as a template in this formula on the basis of which other conditions are compared. It is worth mentioning here, that percentage deviation or error being an old and precise statistical method is used for the purpose of comparison between two values especially between ideal and measured. The proposed energy formulas are validated through some artificially created harmonic signals. Different fault cases are provided by introducing and eliminating some of the specific harmonic contents as shown in Table 5.1. %FS related to these signals are calculated by using equation (23).

Table 5.2 Nomenclature followed in Validation

Nomenclature	Representation
1kAC1	Faulty signal Case 1 sampled at 1kHz
1kAC2	Faulty signal Case 2 sampled at 1kHz
1kAC3	Faulty signal Case 3 sampled at 1kHz
10kAC1	Faulty signal Case 1 sampled at 10kHz
10kAC2	Faulty signal Case 2 sampled at 10kHz
10kAC3	Faulty signal Case 3 sampled at 10kHz

Table 5.2 lists out the nomenclature followed in the validation of the proposed algorithm along with the detailed representations of the same. This nomenclature is followed throughout this chapter in various figures. Faulty signals corresponding to the three different cases have been samples at 1 kHz and 10 kHz and results noted down for each of these cases. The comparison shows that sampling at higher frequency is advantageous and helps to capture more minute details of the fault, thus proving more fruitful for better analysis.

Table 5.3 Frequency Band for Validation for 1 kHz sampling frequency

DWT Nodes	Frequency Band (Hz)
A5	0-15.625
D5	15.625-31.25
D4	31.25-62.5
D3	62.5-125
D2	125-250
D1	250-500

Table 5.4 Frequency Band for Validation for 1 kHz sampling frequency

WPT Nodes	Frequency Band (Hz)
30	0-62.5
31	62.5-125
32	125-187.5

33	187.5-250
34	250-312.5
35	312.5-375
36	375-437.5
37	437.5-500

Table 5.5 Frequency Band for Validation for 10 kHz sampling frequency

DWT Nodes	Frequency Band (Hz)
A5	0-156.25
D5	156.25-312.5
D4	312.5-625
D3	625-1250
D2	1250-2500
D1	2500-5000

Table 5.6 Frequency Band for Validation for 10 kHz sampling frequency

WPT Nodes	Frequency Band (Hz)
30	0-625
31	625-1250
32	1250-1875
33	1875-2500
34	2500-3125
35	3125-3750
36	3750-4375
37	4375-5000

According to Nyquist's theorem, if the original signal is being sampled at f_sHz, the highest frequency that the signal could contain would be $f_s/2$ Hz. In this validation, when the frequency of sampling of the original signal has been taken as first as 1 kHz, the highest frequency in the sampled signal is 500 Hz as shown in the Table 5.3 and Table 5.4 above. And, when the frequency of sampling of the original signal has been taken as first as 10 kHz, the highest frequency in the sampled signal is 5 kHz as shown in the Table 5.5 and Table 5.6 above. In case of sampling at 1 kHz, introduction of up to

the tenth harmonic can be analysed. But, sometimes more parameters may be needed for better analysis. For this, sampling at higher frequency proves to be very useful.

The tables give the complete list of frequency bands for analysis of the artificial signals by the proposed algorithm of Discreet Wavelet Transform and Wavelet Packet Transform. The DWT nodes corresponding to the frequency bands have been assigned the nomenclature as A5, D5, D4, D3, D2 and D1 and the WPT nodes corresponding to the frequency bands have been assigned the nomenclature as 30, 31, 32, 33, 34, 35, 36, 37. This nomenclature is followed in the graphs that depict the results in the further discussion.

5.2 Faulty Case-I (sampling frequency 1 kHz)

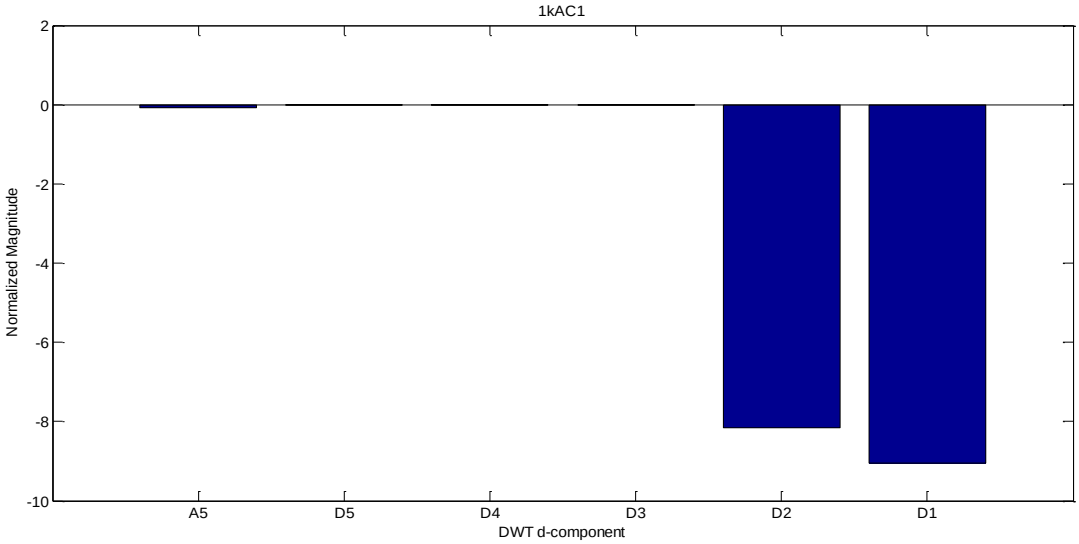

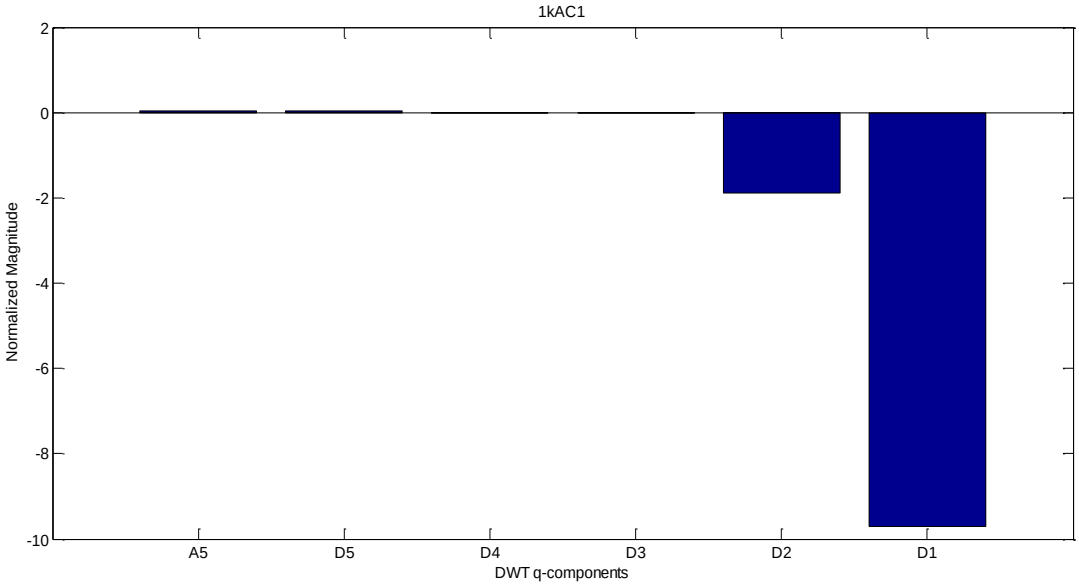

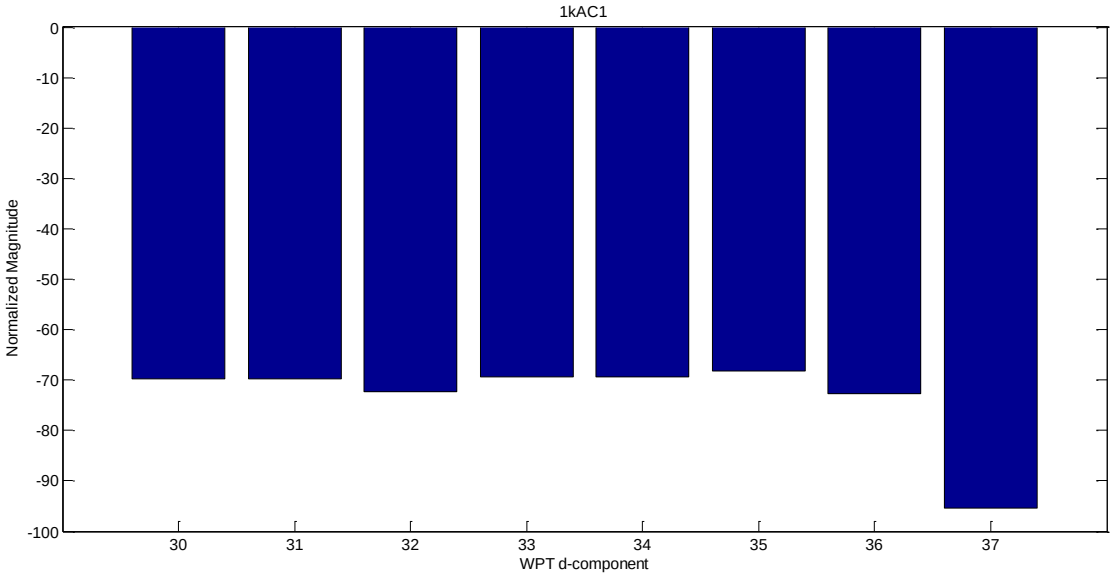

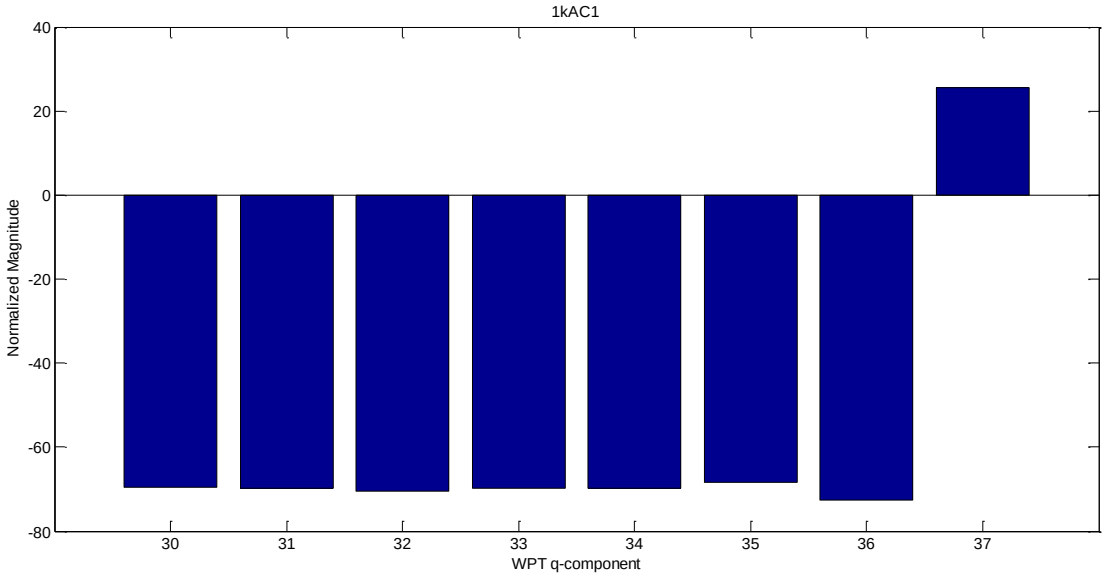

From the above graphs, it is clearly seen that in case of DWT d-components as well as q-components, nodes D1 and D2 are most affected showing deviation in higher frequency components. Also, q-components' D1 node is more affected than d- components'. WPT d-components' all nodes are equally affected except 37 which is the most affected. In WPT q-components, all nodes are equally affected and show negative difference except node 37 being positive with %FS around 20%.

It is found that even the minute changes in magnitude of harmonics are detected by the algorithm. From WPT d-component, thedifference is negative as the frequency component in faulty signal is reduced compared to healthy signal.

5.3 Faulty Case-II (sampling frequency 1 kHz)

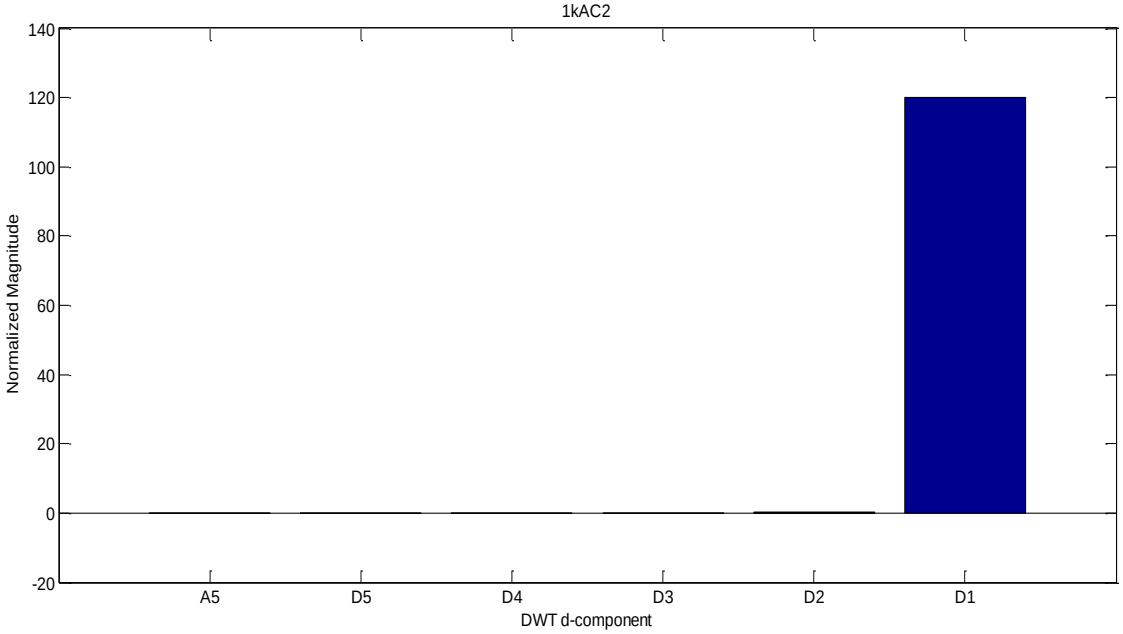

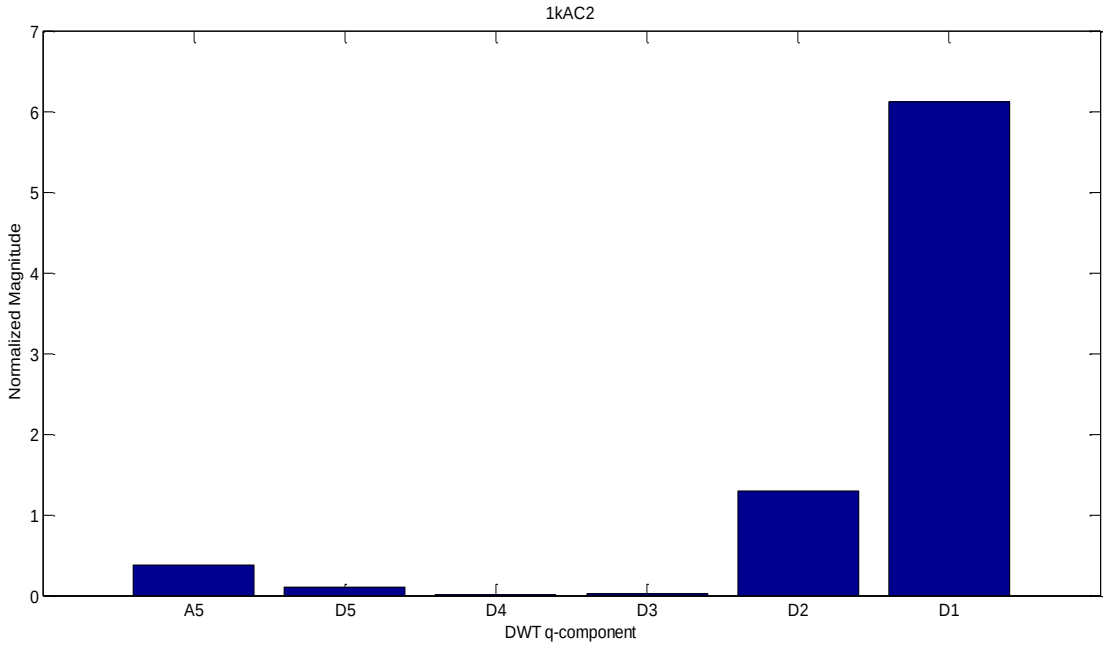

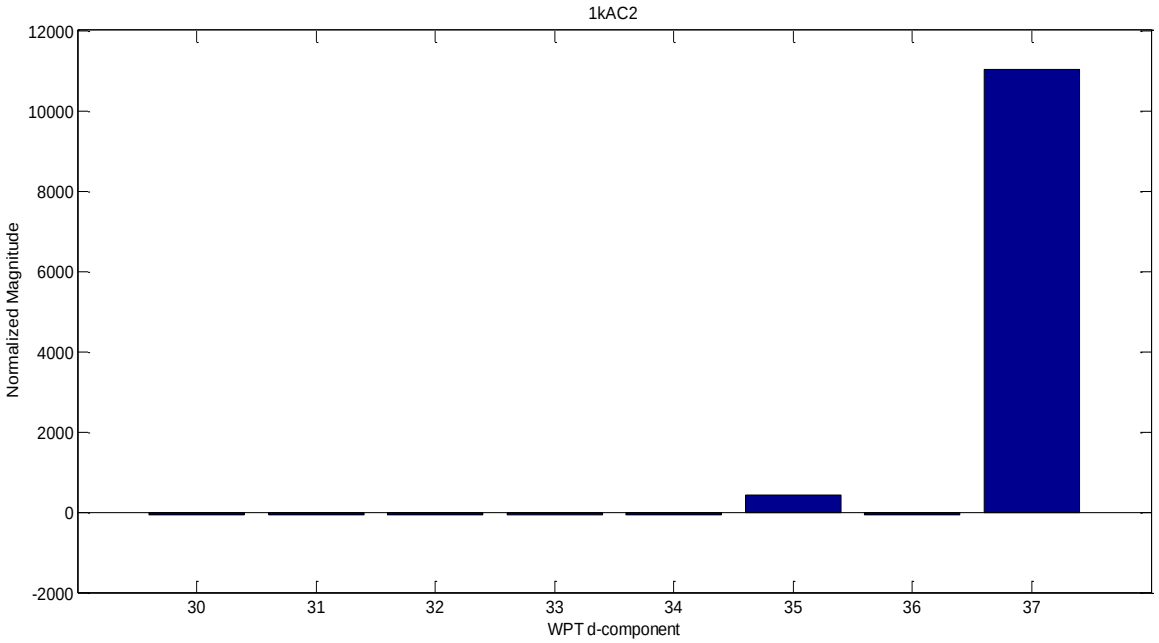

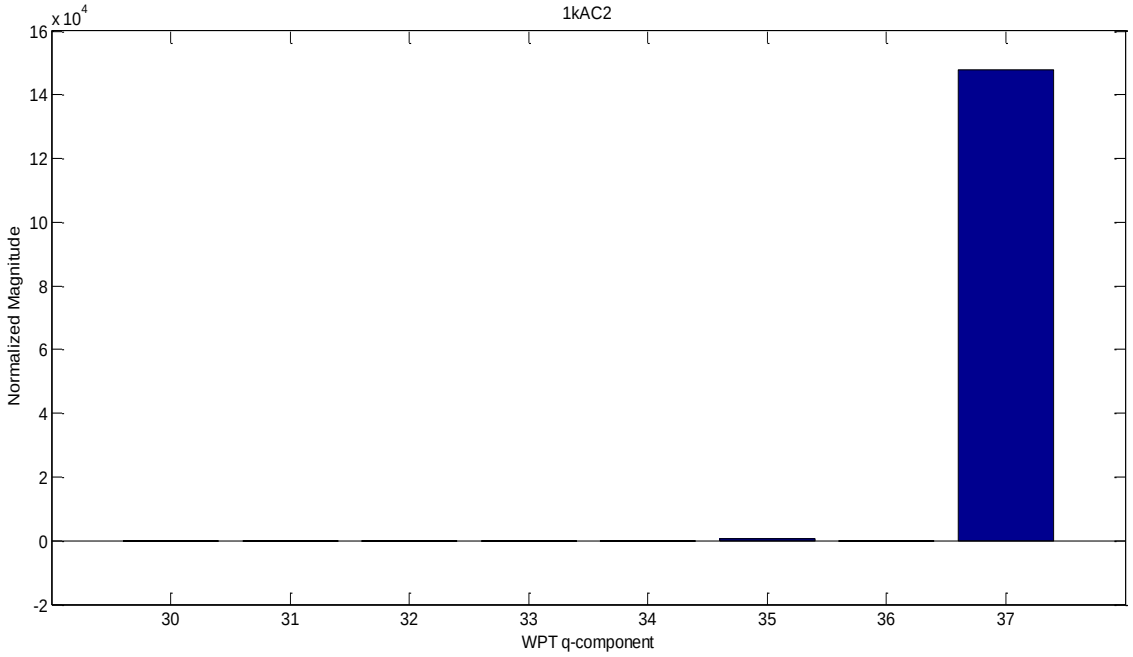

When introduction of seventh harmonics (1kAC2) in faulty signal compared to healthy signal, the D1 node (250-500 Hz) of DWT d-components is most affected. The A5 and D2 nodes of *q*-components are also affected to a small extent with D1 being the most affected one. In WPT *d*-components and q-components, node 37(437.5-500) is most affected and that of q-component is showing larger variation on positive side. Small change on node 35(312.5-375) is also seen.

5.4 Faulty Case-III (sampling frequency 1 kHz)

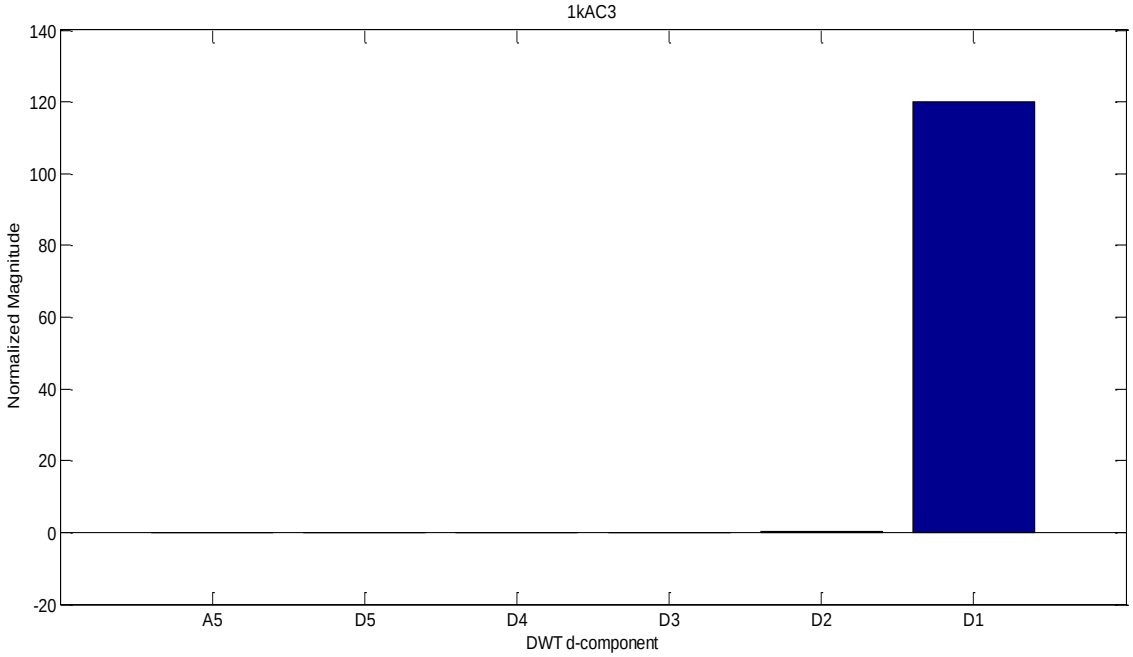

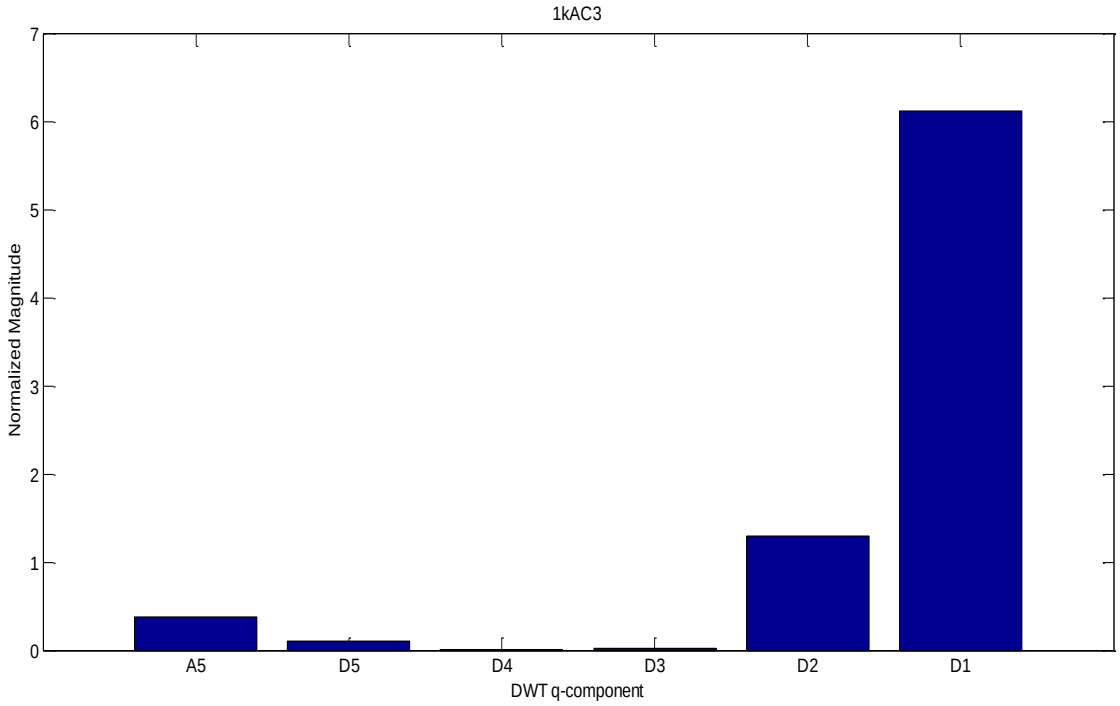

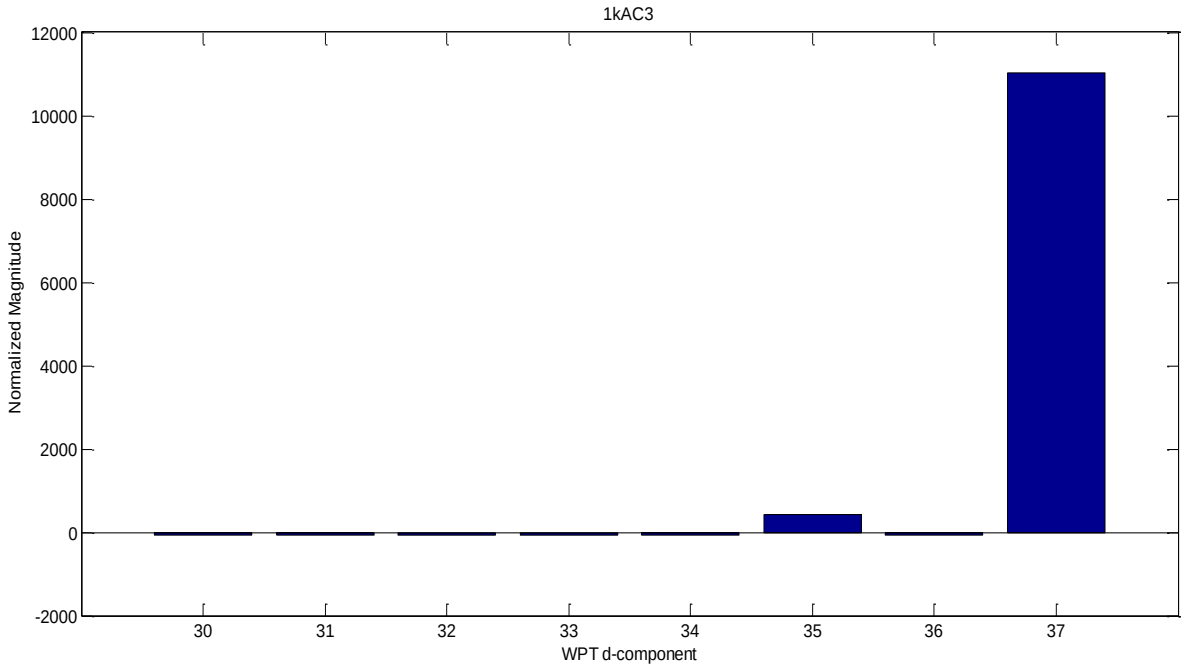

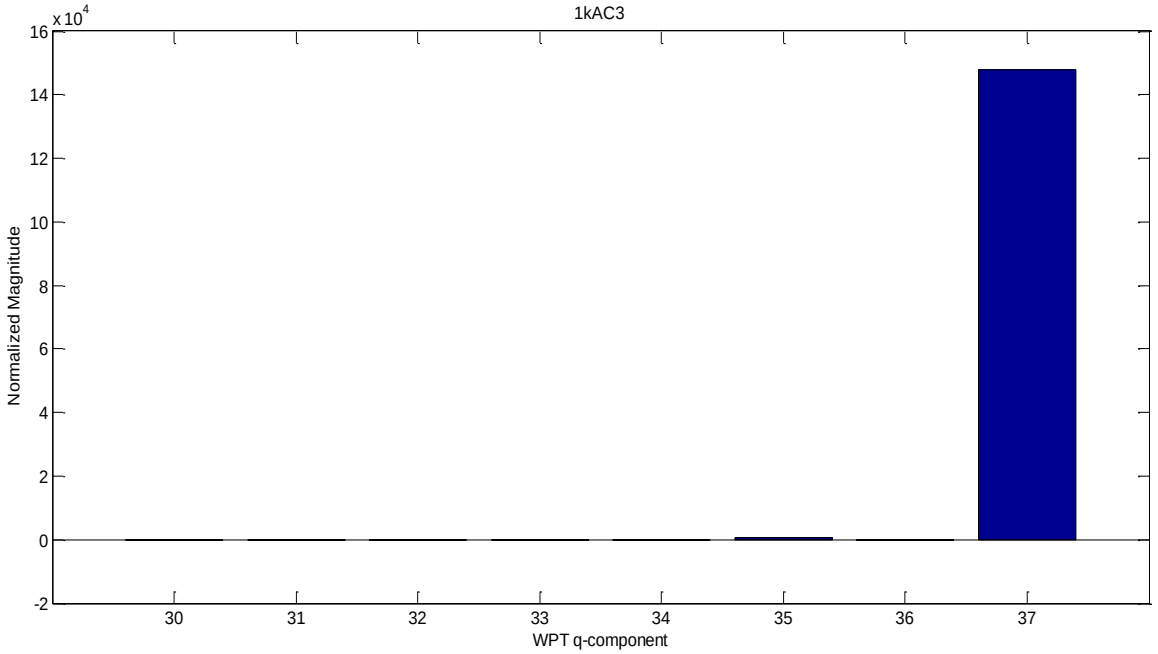

On introducing seventh and ninth harmonics(1kAC3), the DWT d-components show variation in D1 node only while in case of q-components, node D1 is most affected followed by D2, A5 and D5 nodes which are less affected. The node 37 (437.5-500 Hz) of WPT d-components and q-components is vastly affected with 35 (312.5-375) being minutely affected. Comparison with the previous case shows that on introducing higher harmonics, the corresponding band is more affected in magnitude. Also, very small change is also easily detected.

5.5 Faulty Case-I (sampling frequency 10 kHz)

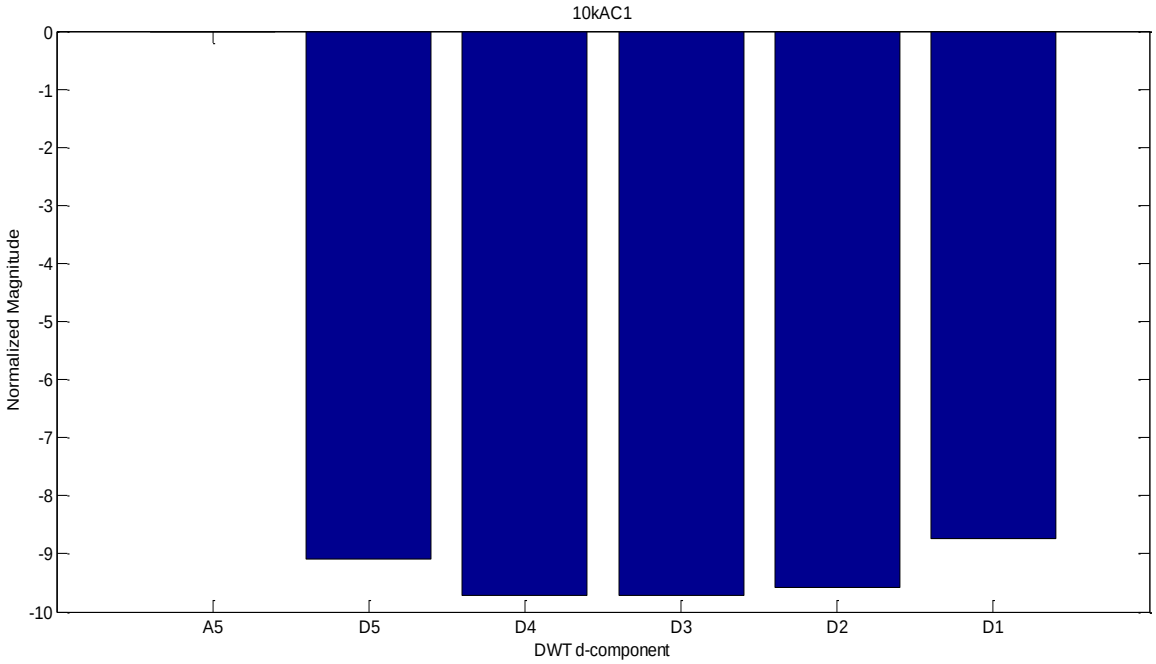

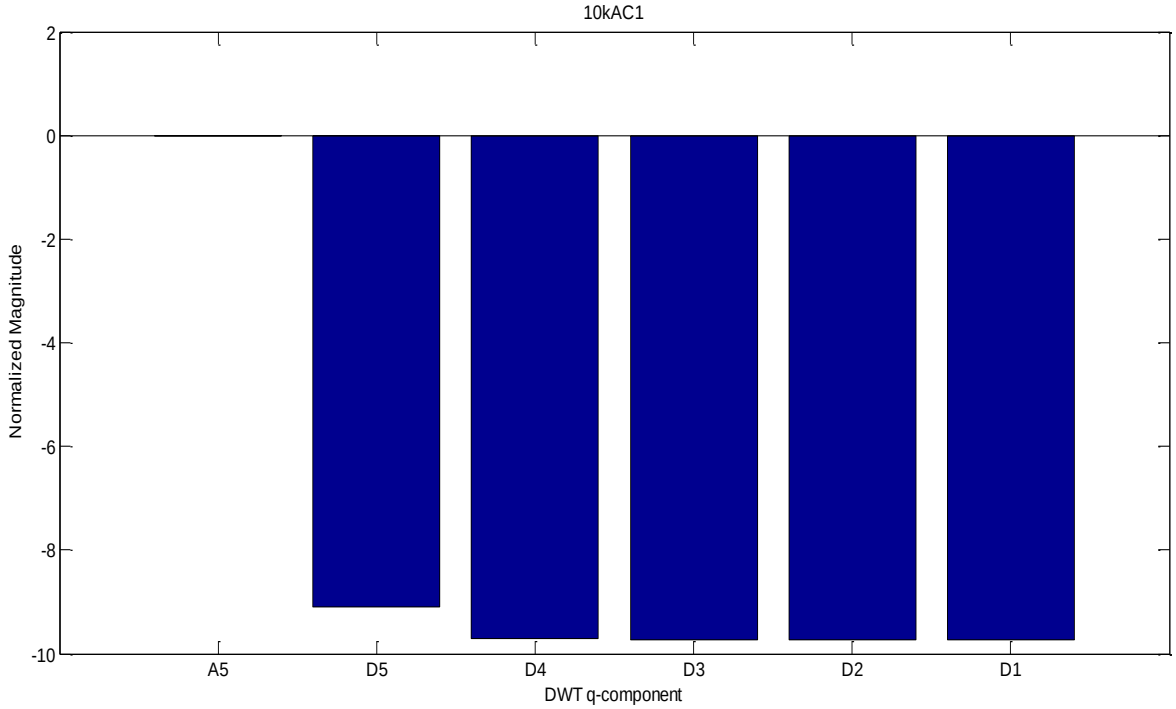

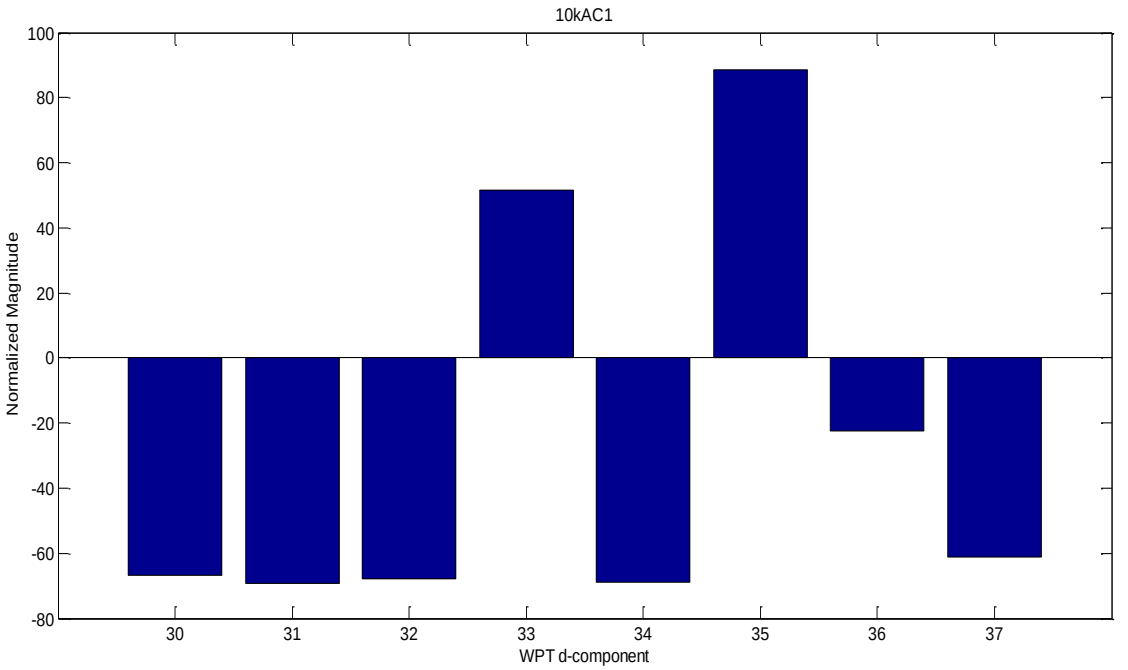

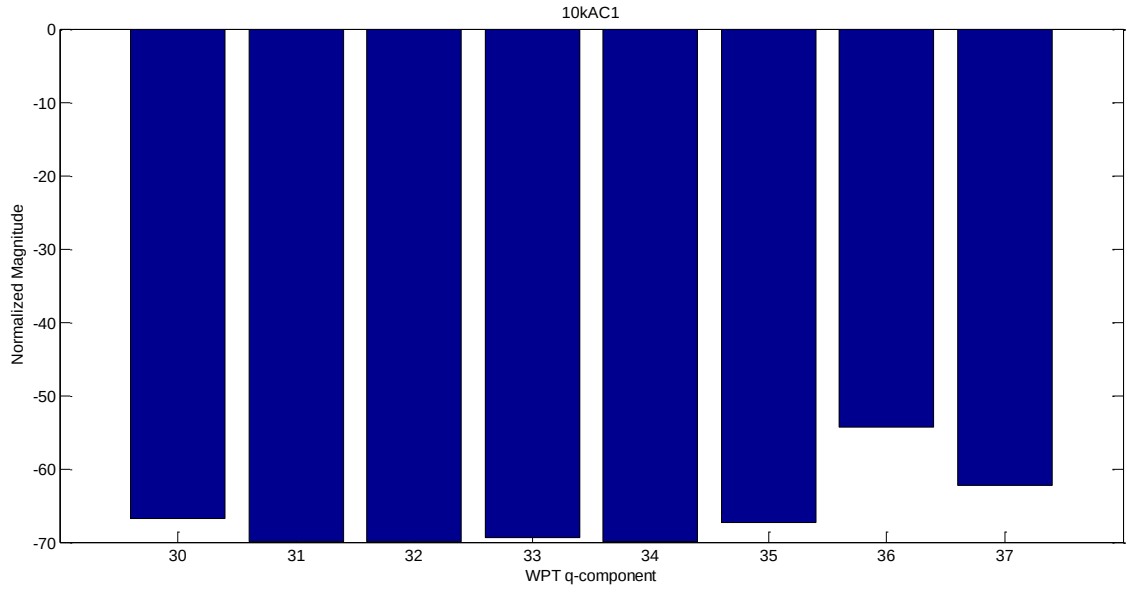

For the signals sampled at 10 kHz for faulty case in which third harmonic is increased and fifth harmonic is increased minutely, the D2, D3 and D4 nodes of DWT d and q- components show similar trends with %FS being nearly 95% on negative side. In DWT d-component, D5 and D1 follow next with %FS being 90%. In DWT q-component, node D1 is same as other nodes followed by node D5. The WPT d-components' nodes show negative %FS equal to 70% except node 35 showing positive %FS equal to 90% followed by nodes 33 and 36. % FS of all nodes in WPT q-components is negative. Node 36 shows minimum variation followed by 37. Here, q-components are more affected compared to d-components.

5.6 Faulty Case-II (sampling frequency 10 kHz)

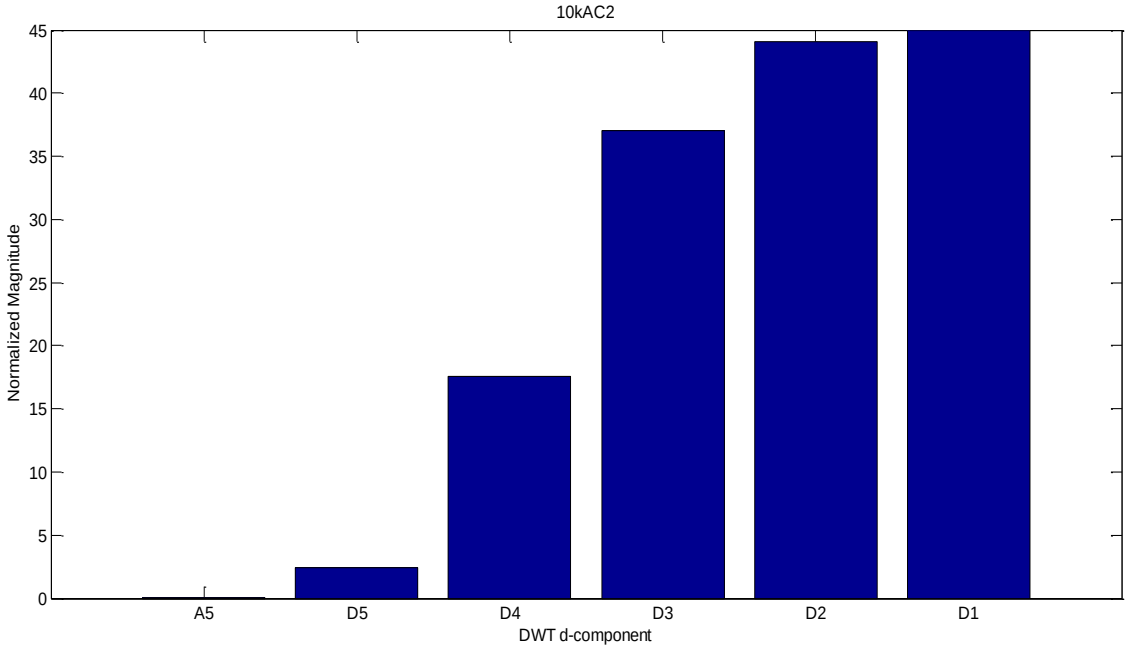

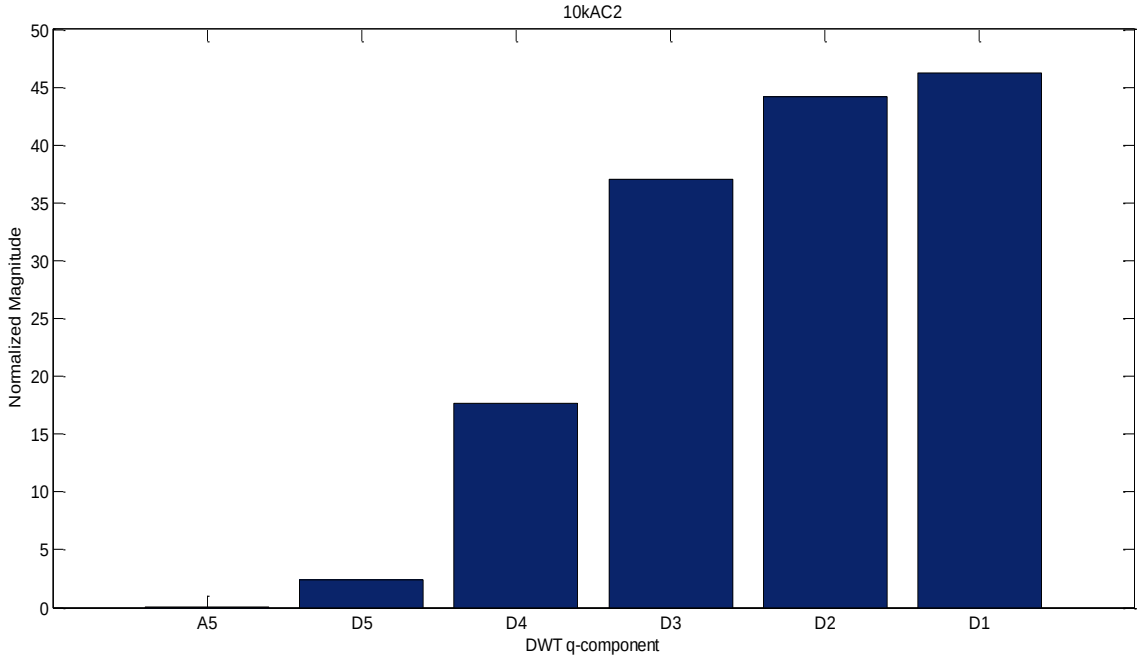

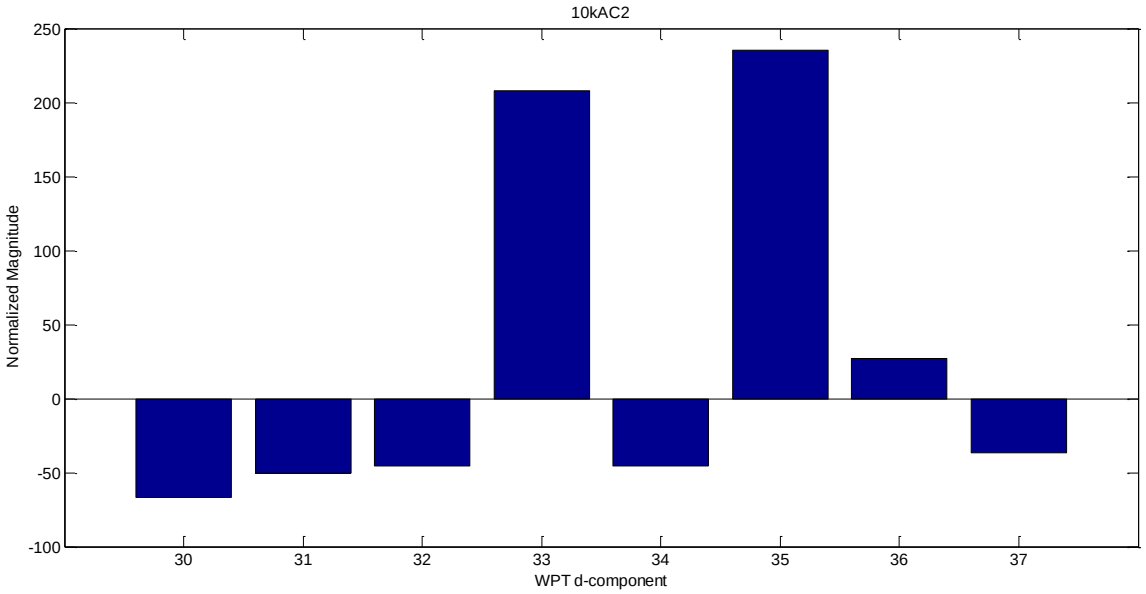

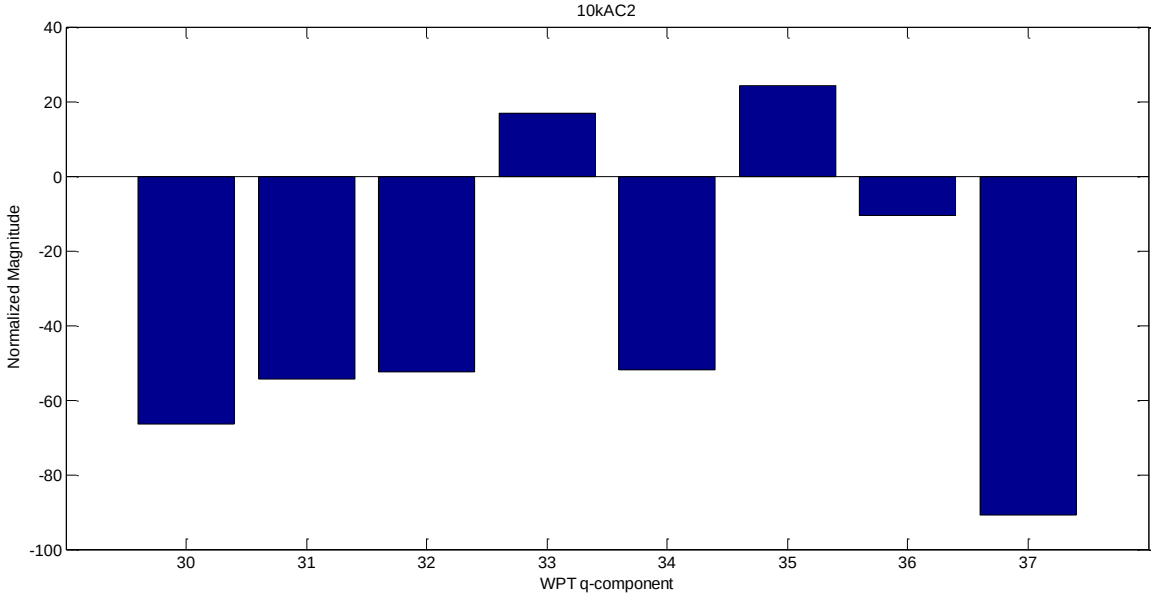

For the faulty case of introduction of seventh harmonic and the signals being sampled at 10 kHz(10kAC2),the DWT d and q-components' are affected similarly with node D1 being the most affected one followed by D2, D3, D4 and D5. For WPT q-components, node 35 is most affected on positive side followed by 33 with small effect on 36. Rest of the nodes are negatively affected with node 30 being the most. The WPT components show negative deviation in all nodes except 33 and 35 with %FS of 37 being 90% followed by 30(about 70%) and the rest having % FS nearly 50%.

Looking at WPT q-components, it seems that node 30 (0-625 Hz) is the affected one but this is a wide region. On further increasing the frequency resolution of lower frequencies via DWT, It is evidentthat A5 and D5 are not affected and D4 is very little affected. Also, DWT shows that D1

(2500-5000 Hz) is most affected. Again, for DWT this is a wide region. On looking at equally bifurcated smaller regions of WPT helps to conclude node 37 (4375-5000 Hz) being the most affected one.This particular situation shows that selection of DWT or WPT is based on frequency range and resolution required to capture the information required.

5.7 Faulty Case-III (sampling frequency 10 kHz)

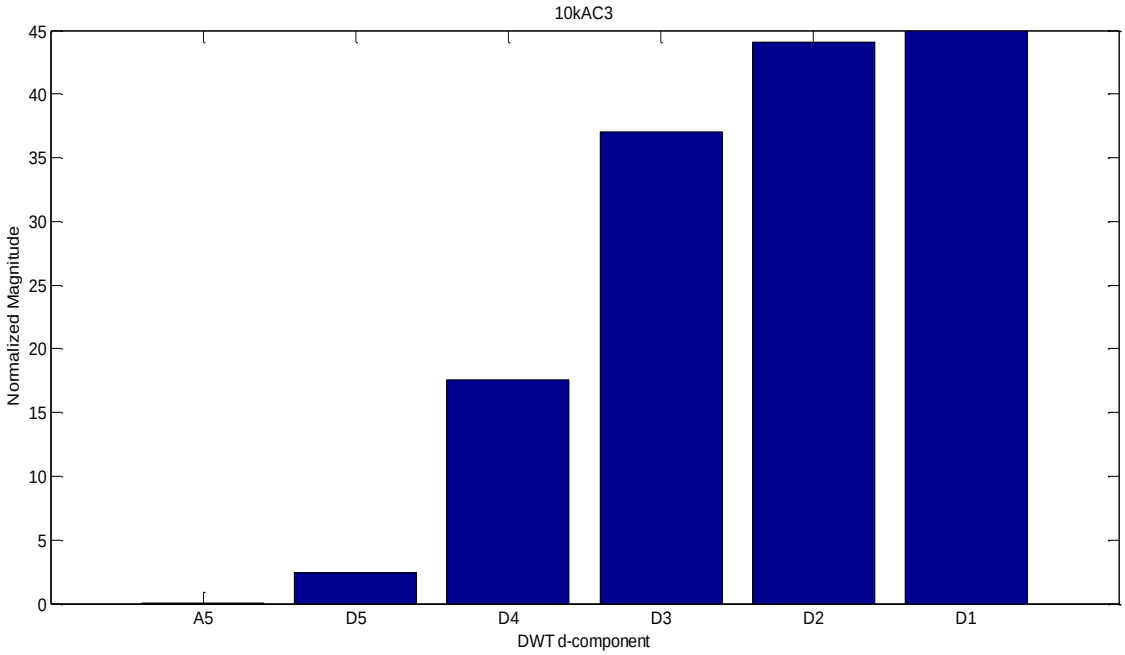

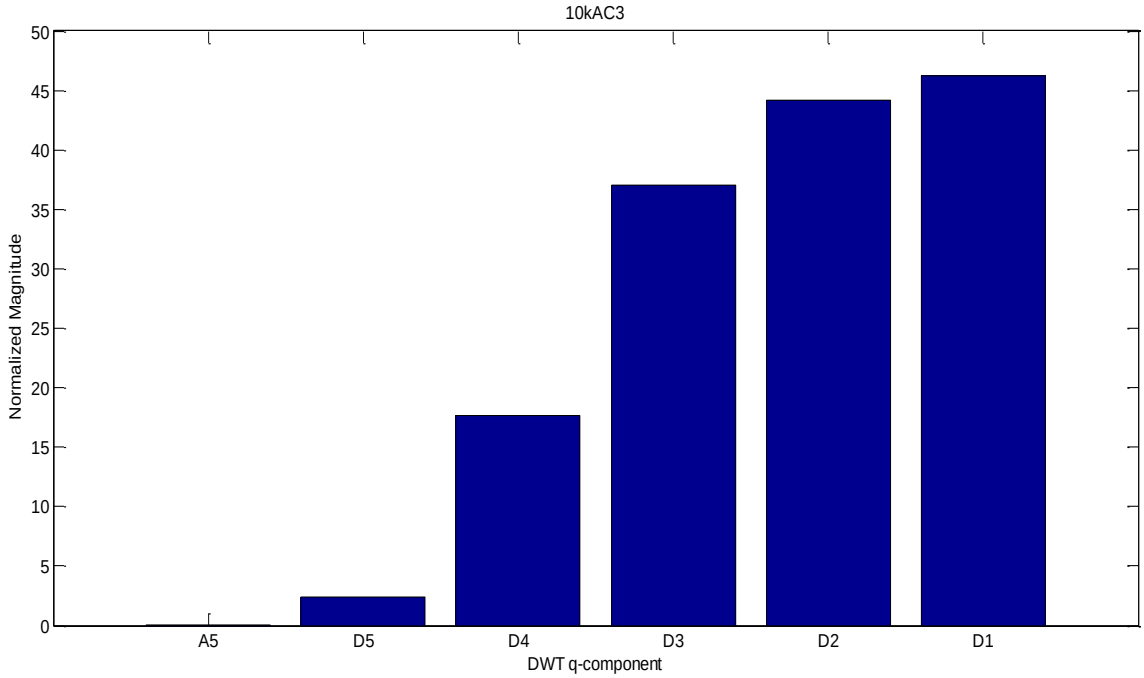

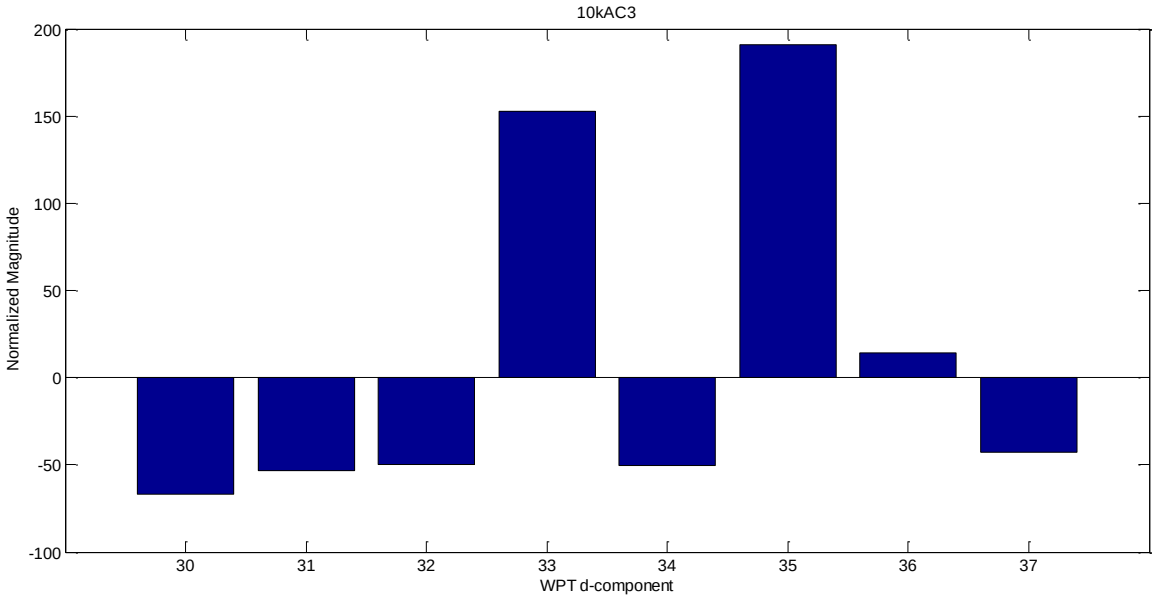

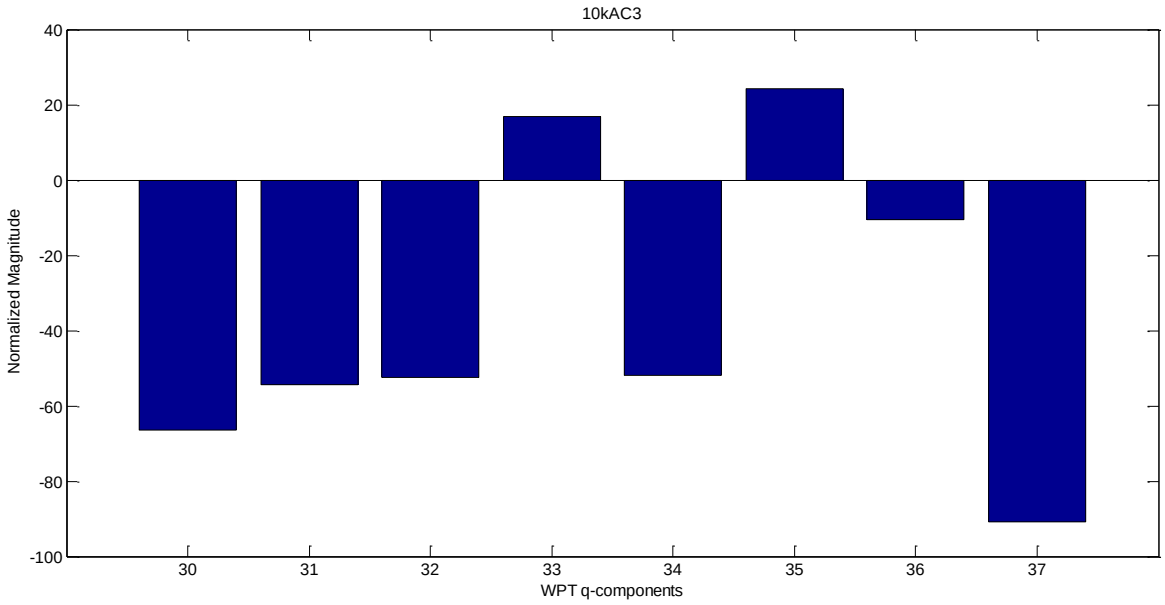

For introduction of seventh and ninth harmonics and sampling at 10 kHz, the DWT d-components shows similar variation in decreasing order of nodes D1, D2, D3, D4, D5, A5. In WPT d-components, most affected node is 35 followed by 33, both on positive side with 36 having small % FS. Node 30 is affected most in negative side followed by remaining nodes.In WPT q-components, most affected node is 37 followed by 30, 31, 32 and 34 on negative side. Node 35 shows most effect on the positive side with 33 close behind. Even small changes in the harmonics compared are detected. Compared to the previous case, the similar combination of bands is affected with the magnitude differing slightly.

In this context, it is evident that the graphs obtained are not of actual phase currents but from their d-q transformations, which are related to the magnetic properties, bearing no relation, whatsoever, the phase currents. Also, redistribution of energy takes place among different nodes in the algorithm and mere looking at the current equations does not give an idea of the frequency that would be most affected. The motto of the algorithm is to detect occurrence of faults in their nascent stages and not at all relates to the frequency that is affected due to fault.

It can be verified that for faulty case II and III, the introduction of higher order harmonics increase the %FS very significantly.Comparative study of faulty caseII and III validates the fact that after applying d-q transform, frequency band selection for a particular signature cannot be governed theoretically since energy is distributed throughout the range, and this reasons for greater emphasis on the importance of proposed work.

Change in different parameters affects different frequency ranges. Severity of fault can be judged by the practically observed fact that as severity increases, higher order frequency ranges viz. 1250-2500 Hz, 2500-5000Hz get affected significantly.

Also all faults contain some out-of-box results like reduction in difference of signal energies in case of some fault. This can be a major hurdle for the identification of fault. This drives us to an important conclusion that physical observation and expert systems applied on signal energies calculated for such worst conditions can’t fulfil the purpose of fault classification. Nevertheless, it is clear that this algorithm is sufficient for fault detection purpose.

Signal energy is a parameter independent of the nature of signal. It gives an idea about the energy required for signal to maintain its existence in nature. So the current signal energy can serve as an excellent tool of MCSA. In this report, analysis of faults gives clear indication that due to the faults, change in magnetic flux, air gap eccentricity, rotor resistance, and friction in bearings cause change in current signal energy.

Chapter 6

Results and Discussion

6.1 Introduction

The aim of this thesis is to advance the field of condition monitoring and fault diagnosis in induction motor operating in variety of operating conditions. The fast growth in applications of the induction motor in sensitive areas as nuclear power plants has increased the need for continuous condition monitoring of motors. The reflection of fault on frequency spectrum is depicted by plotting the normalized energies of stator current signal with frequencies itself. The variation shown here for the actual signals* directly points the severity and the frequency spread of that fault.

Table 6.1 Frequency Band for analysis by DWT

DWT Nodes	Frequency Band (Hz)
A5	0-156.25
D5	156.25-312.5
D4	312.5-625
D3	625-1250
D2	1250-2500
D1	2500-5000

Table 6.2 Frequency Band for analysis by WPT

WPT Nodes	Frequency Band (Hz)
30	0-625
31	625-1250
32	1250-1875
33	1875-2500
34	2500-3125
35	3125-3750
36	3750-4375
37	4375-5000

*obtained from the author of "Bearing Fault Analysis by Signal Energy Calculation based Signal Processing Technique in Squirrel Cage Induction Motor"[63]

6.2 Bearing Fault analysis by DWT

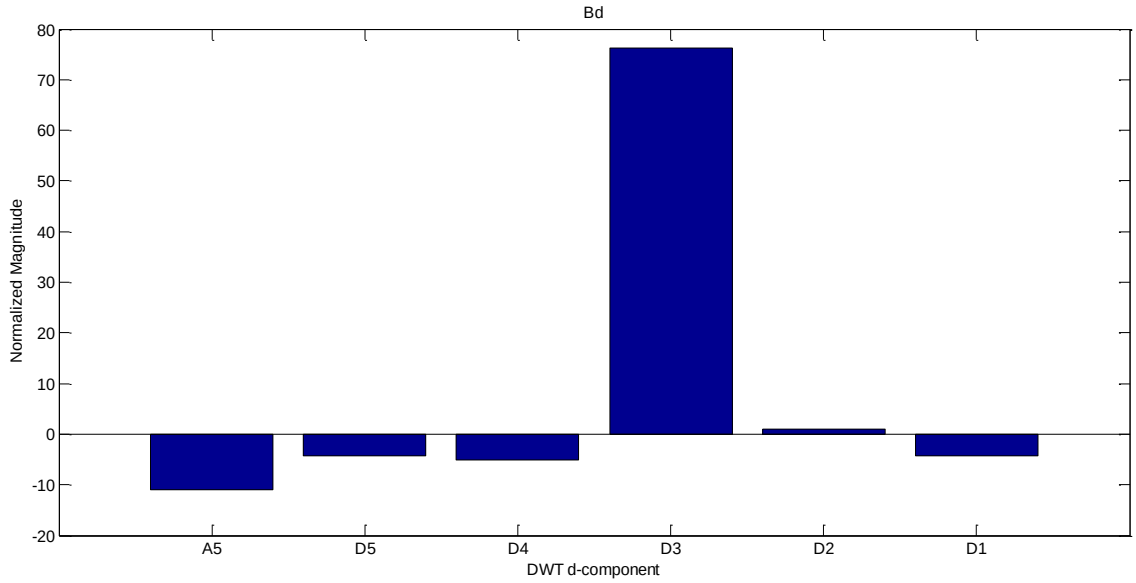

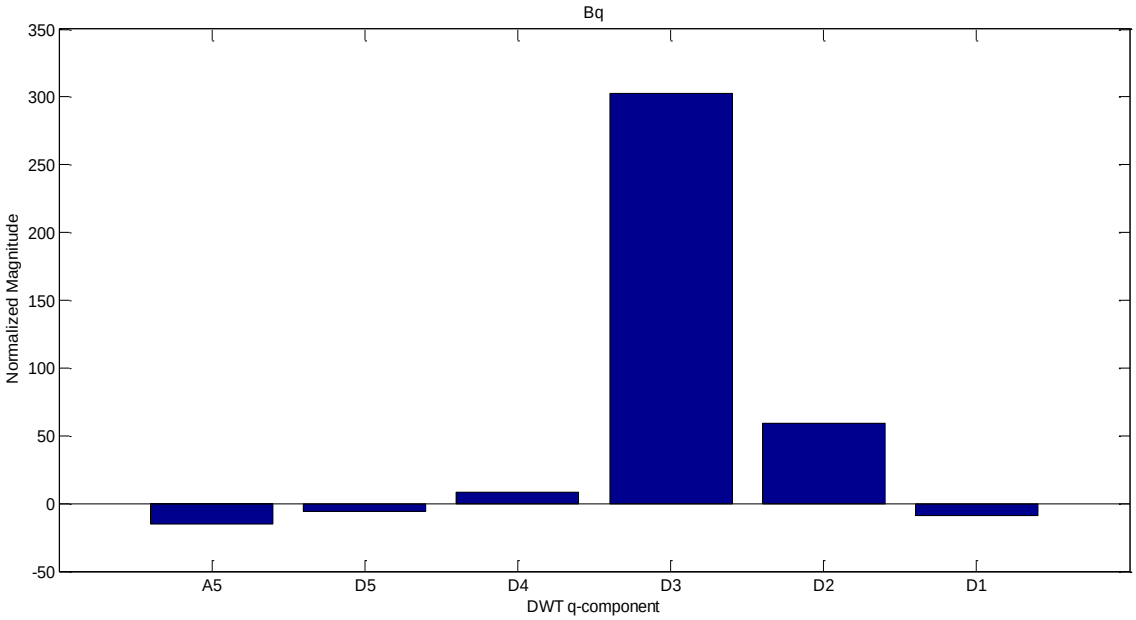

In case of d-components, maximum change is seen in D3 (625-1250 Hz) and %FS is positive implying introduction of new frequency in this range due to fault. All coefficients below 625 Hz (A5, D5, D4) have negative %FS which is surprising. This is because the supply harmonics of lower order get reduced due to the bearing fault. In bearing fault, q- component is affected more than d-component. The maximum change is notable in the same range. %FS increases 3-4 times in comparison to d-component in D3.

6.3 Bearing Fault analysis by WPT

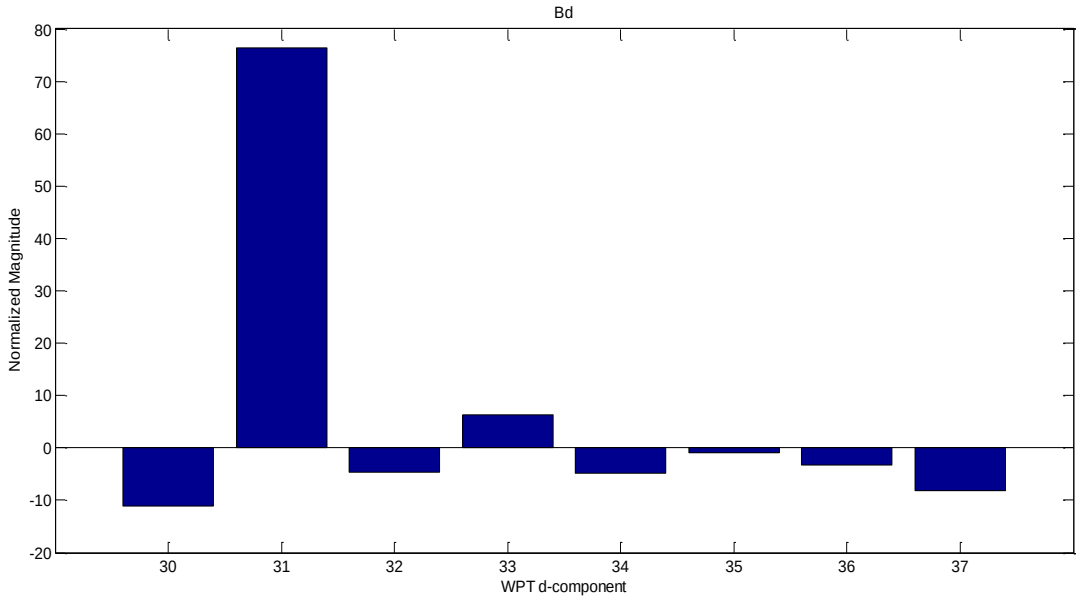

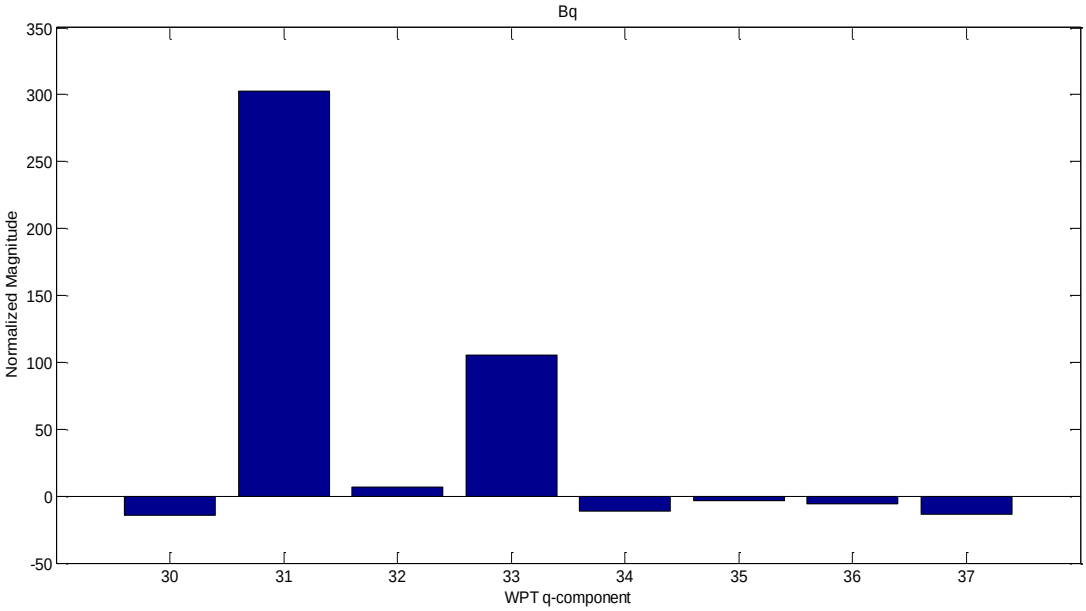

Major change is seen in component 31 (625-1250 Hz) in case of d-components. The lower frequency coefficient (30) has negative %FS.Bearing fault, being a mechanical fault, the %FS in case of q-component increases 3-4 times. Component 30 is most affected. Component 33 is also significantly affected. This is in the range of 1875-2500 Hz.

6.4 Rotor-Cut Fault analysis by DWT

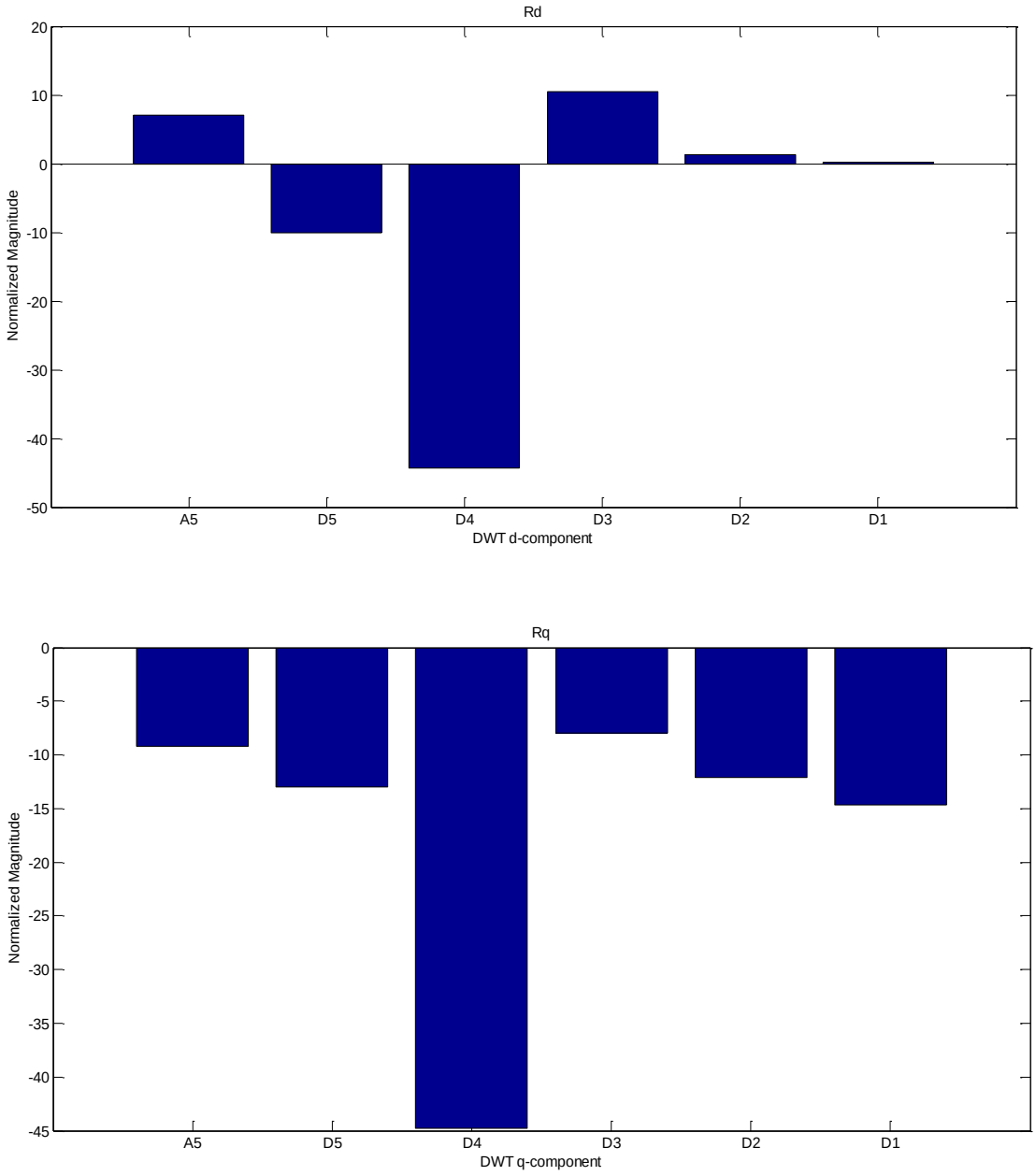

In case of d-components, major change is seen in D4 (312.5-625 Hz) which is closer to the power frequency in comparison to the bearing fault affected coefficient. Negative % FS reflects harmonic elimination. In q-components, all components are negative. Major change is again seen in D4.

6.5 Rotor-Cut Fault analysis by WPT

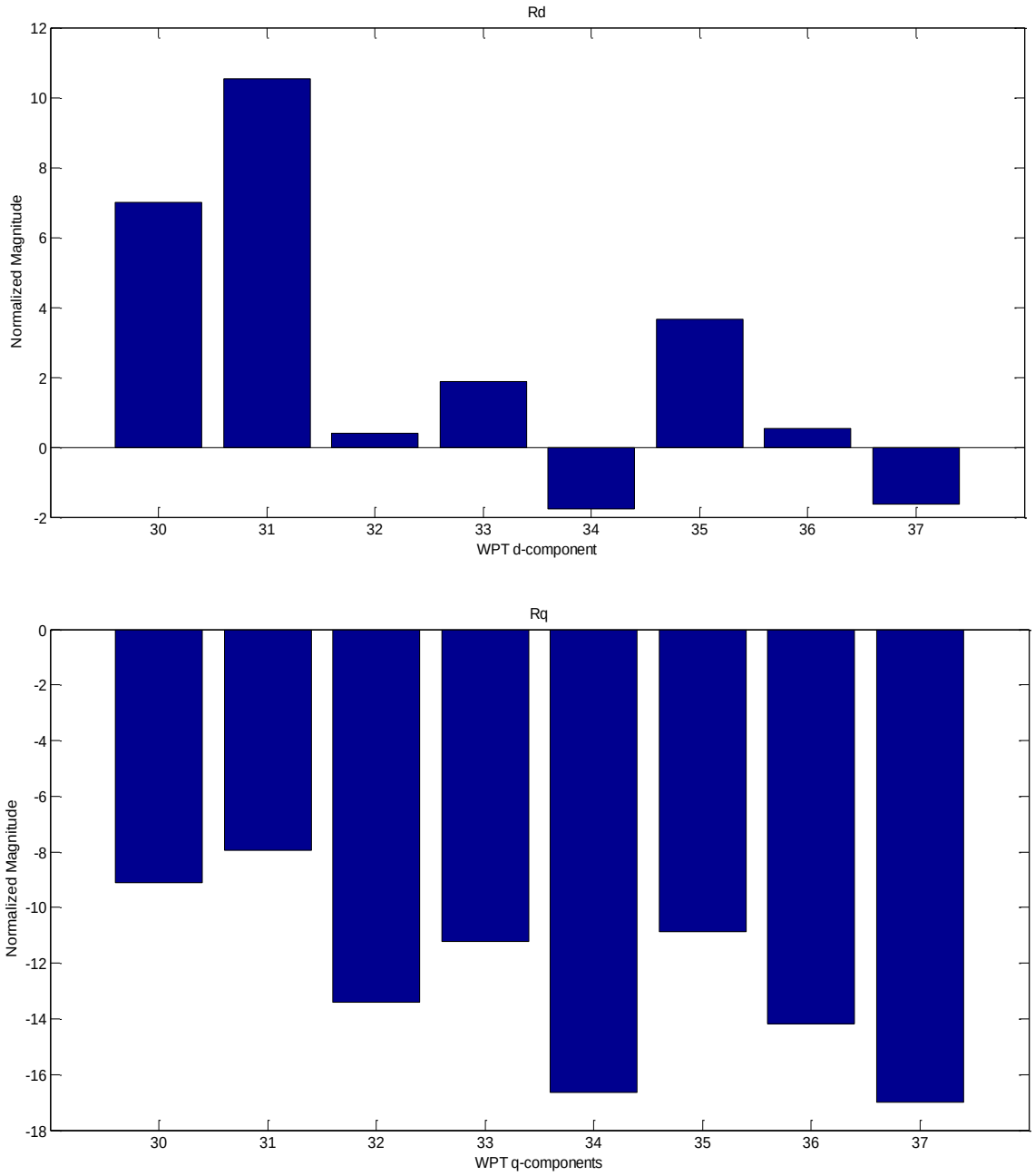

In d- components, 31 is most affected but %FS is around 10% only which is minimum compared to most affected coefficient of other fault cases. Component 30 also gets affected significantly. Higher range coefficient 35 (3125-3750 Hz) also gets affected with %FS around 40% of component 31. The component 33 is affected to a degree of around 17% of component 31. The components 34 and 37 are also affected by the same amount as component 33 but in these, frequencies in the range of 2500-3125 Hz and 4375-5000 Hz respectively are eliminated as compared to healthy signal, therefore, the change is negative.

In case of q-components, 34 and 37 are most affected followed by 32 and 36. All coefficients' %FS is negative due to elimination of some frequencies. Trend is same as of DWT analysis for same fault's same axis current.

Table 6.3 Most Affected Frequency Bands (DWT) for Various Operating Conditions

FAULT TYPE	FREQUENCY BAND(Hz)	
	D-Component	Q-Component
Bearing fault	625-1250	625-1250
Rotor cut fault	312.5-625	312.5-625

Table 6.4 Most Affected Frequency Bands (WPT) for Various Operating Conditions

FAULT TYPE	FREQUENCY BAND(Hz)	
	D-Component	Q-Component
Bearing fault	625-1250	625-1250
Rotor cut fault	625-1250	4375-5000

6.6 Discussion

In case of rotor faults, fault signature was also found forhigher frequencies. Being an electrical fault, in this case, both elimination as well as introduction of harmonics is much lesser than bearing fault. This is due to the fact that rotor cut fault does not affect the air gap flux and air gap magnetic field.

All these reasons forced us to move on to WPT. WPT is a tool for equal emphasized analysis for entire frequency range. In a three level WPT tree, the bandwidth of each coefficient remains same and that is of 625 Hz.

As our data signal is sampled at 10 kHz sampling frequency, we are getting the results for the frequency up to 5000 Hz. In DWT, coefficient D1 takes into account frequency range 2500-5000 Hz while this range is eventually segregated into equally spaced four different coefficients in WPT. This in turn gives a big advantage compared to DWT.

Near power frequency 50 Hz, analysis is more suited by DWT as it gives excellent and desired frequency resolution for lower frequencies. Problem with %FS related to fundamental, third and fifth harmonics is that change in these components is quite obvious and hence cannot be used for fault identification and classification. DWT coefficient D3 has a unique similarity with its counterparts that it also has a bandwidth of frequency 625 Hz. By observing the analysis of bearing fault in both

DWT and WPT, it can be seen that major change arrives in D3 or 31 component as both carry same 625-1250 Hz frequency.

6.7 Future Expansion

In the work done above, a base algorithm is discussed for detection of faults in induction motor at different operating conditions. This algorithm might be useful in industries for detecting fault which will save time and money as well. Sampling at higher frequencies, though increases the parameters for analysis but also increases the complexity of the algorithm and may take time in calculation. There is no specified set of rules or formulae regarding this and calls for large number of cases to make a better judgement. This calls for a scope of future expansion of this work.

References

[1] R.A. Gupta, A.K. Wadhwani, and S.R. Kapoor, "Early Estimation of Faults in Induction Motors Using Symbolic Dynamic-Based Analysis of Stator Current Samples", *IEEE Transactions onEnergy Conversion,* vol. 26, no.1, pp. 102-114, March 2011

[2] Austin H. Bonnett and Tim Albers, "Squirrel Cage Rotor Options for A.C. Induction Motors", *IEEE Transactions on Industry Applications*, vol. 37, issue: 4, pp. 1197-1209, July/ August 2002.

[3] Austin H. Bonnett and T. Albers, "Squirrel-Cage Rotor Options for AC Induction Motors", *IEEE Transactions Industry Applications,* vol. 37, no. 4, pp. 1197-1209, July/ August 2001.

[4] Jee-Hoon Jung, Jong-Jae Lee, and Bong- Hwan Kwon, "Online Diagnosis of Induction Motors Using MCSA", *IEEE Transactions on Industrial Electronics,* vol. 53, no. 6, pp. 1842-1852, December 2006.

[5] M. E. H. Benbouzid, "A Review of Induction Motors Signature Analysisas a Medium for Faults Detection", *IEEE Transactions on Industrial Electronics*, vol. 47, no. 5,pp. 984–993, Oct. 2000.

[6] Subhasis Nandi, H. A. Toliyat, and Xiaodong Li, "Condition Monitoring and Fault Diagnosis of Electrical Motors- A Review", *IEEE Transactions on Energy Conversion,* vol. 20, no. 4, pp. 719-729, December 2005.

[7] M.E.H. Benbouzid and G.B. Kliman, "What Stator Current Processing-Based Techniques to Use for Induction Motor Rotor Fault Diagnosis?",*IEEE Transactions on Energy Conversion,* vol. 18, no. 2, pp. 238-244, June2003.

[8] DebasmitaBasak, ArvindTiwari, and S. P. Das, "Fault Diagnosis and Condition Monitoring of Electrical Machines- A Review", *IEEE International Conference on Industrial Technology,* pp. 3061-3066, 15-17 Dec. 2006, Mumbai.

[9] Subhasis Nandi and Hamid A. Toliyat, "Fault Diagnosis of Electrical Machines- A Review", *IEEE International Conference on Electric Machines and Drives,* pp. 219-221, 9-12 May 1999, Seattle, WA.

[10] Austin H. Bonnett, "The Benefits of Allowing for Increased Starting Current in A.C. Squirrel/ Cage Induction Motors", *IEEE Industry Application Society 37th Annual Petroleum and Chemical Industry Conference,* pp. 93-98, 10-12 Sept. 1991, Houston, TX.

[11] M.E.H. Benbouzid, "Bibliography on Induction Motor Faults Detection and Diagnosis", *IEEE Transactions on Energy Conversion,* vol. 14, no. 4, pp. 1065-1074, December 1999.

[12] P. J. Tavner, "Condition monitoring—The way ahead for large electrical machines", in *Proceedings of IEEE International Conference on Electrical Machines and Drives*, pp. 159–162, 1989, London, U.K.

[13] Subhasis Nandi and Hamid A. Toliyat, "Condition Monitoring and Fault Diagnosis of Electrical Machines- A Review", *IEEE 34th IAS Annual Meeting, Industry Applications Conference,* vol. 1, pp. 197-204, 3-7 Oct. 1999, Phoenix, AZ.

[14] ShahinHedayatiKia, HumbertoHenao, and Gérard-André Capolino, "Efficient Digital Signal Processing Techniques for Induction Machines Fault Diagnosis", *IEEE Workshop on Electrical Machines Design Control and Diagnosis,* pp. 232-236, 11-12 March 2013, Paris.

[15] *http://en.wikipedia.org*

[16] M. E. H. Benbouzidet. al., "Induction Motors Faults Detection and Localization Using Stator Current Advanced Signal Processing Techniques", *IEEE Transactions on Power Electronics,* vol. 14, no. 1, pp. 14–22, Jan. 1999.

[17] M.E.H. Benbouzid and R. Beguenane, "Induction Motors Thermal Monitoring by Means of Rotor Resistance Identification", *IEEE Transactions on Energy Conversion,* vol. 14, no. 3, pp. 566-570, Sept. 1999.

[18] Alberto Bellini, Fabio Immovilli, Riccardo Rubini and Carla Tassoni, "Diagnosis of Bearing Faults in Induction Machines by Vibration or Current Signals: A Critical Comparison", *IEEE Transactions on Industry Applications,* vol. 46, issue: 4, pp. 1350-1359, July-August 2010.

[19] Mariana Iorgulescu, and Robert Beloiu, "Vibration and Current Monitoring for Fault's Diagnosis of Induction Motors", *Annals of the University of Craiova,* Electrical Engineering Series, no. 32,pp. 102-107, 2008. ISSN: 1842-4805.

[20] J. R. Cameron, W. T. Thomson, and A. B. Dow, "Vibration and Current Monitoring for Detecting Air-gap Eccentricity in Large Induction Motors", *Proceedings of Electrical Engineering,* vol. 133, pt. B, pp. 153-163, May 1986.

[21] Basel Isayed et.al. , "Vibration Monitoring and Faults Detection Using Wavelet Techniques", *IEEE 9th International Symposium on Signal Processing and Its Application, ISSPA,* pp. 1-4, 12-15 Feb. 2007, Sharjah.

[22] P. J. Tavner, K. K. Amin, and C. Hargis, "An electrical technique for monitoring induction motor cages", in *Proceedings IEEE Int. Conf.onElectrical Machines and Drives*, London, U.K., pp. 43–46, 1987.

[23] R.R. Schoen, T.G. Habetler, F. Kamran and R.G. Bertheld, "Motor Bearing Damage Detection Using Stator Current Monitoring", *IEEE Industry Applications Society Meeting,* pp. 110-116, 2-6 Oct. 1994, Denver, CO.

[24] Ramzy R. Obaid, Thomas G. Habetler, and Jason R. Stack, "Stator Current Analysis for Bearing Damage Detection in Induction Motors", *4th IEEE International Symposium on Diagnostics for Electric Machines, Power Electronics and Drives,* pp. 182-187, 24-26 Aug. 2003.

[25] NeelamMehala, RatnaDahiya, "Motor current signature analysis and its applications in Induction Motor Fault Diagnosis"*, International Journal of Systems Application,* Engineering Development, vol. 2, issue 1, pp. 29-35, 2007.

[26] M.E.H. Benbouzid, H. Nejjari, R. Beguenane and M. Vieira, "Induction Motor Asymmetrical Faults Detection using Advanced Signal Processing Techniques", *IEEE Transactions on Energy Conversion,* vol. 14, no. 2, pp. 147-152, June 1999.

[27] M. Ikeda and T. Hiyama, "Simulation Studies of the Transients of Squirrel-Cage Induction Motors", *IEEE Transactions on Energy Conversion,* vol. 22, no. 2, pp. 233-239, June 2007.

[28] James W. Cooley, Peter A. W. Lewis, and Peter D. Welch, "The Fast Fourier Transform and its Applications", *IEEE Transactions on Education*, vol. 12, no. 1, pp. 27-34, March 1969.

[29] M. Riera-Guaspet. al., "Diagnosis of Induction Motor Faults via Gabor Analysis of the Current in Transient Regime", *IEEE Transactions on Instrumentation and Measurement,* vol. 61, no. 6, pp. 1583-1596, June 2012.

[30] H. Nejjari and M.E.H. Benbouzid, "Monitoring and Diagnosis of Induction Motors Electrical Faults Using a Current Park's Vector Pattern Learning Approach", *IEEE Transactions on Industry Applications,* vol. 36, issue: 3, pp. 730-735, May/ June 2002.

[31] H. Nejjari and M.E.H. Benbouzid, "Monitoring and Diagnosis of Induction Motors Electrical Faults Using a Current Park's Vector Pattern Learning Approach", *IEEE Transactions on Industry Applications,* vol. 36, no. 3, pp. 730-735, May/ June 2000.

[32] Samira Ben Salem, WalidTouti, KhmaisBacha, and AbdelkaderChaari, "Induction Motor Mechanical Fault Identification Using Park's Vector Approach", *IEEE International Conference on Electrical Engineering and Software Applications,* pp. 1-6, 21-23 March 2013, Hammamet, Tunisia.

[33] AbithaMemala. W and Dr. V. Rajini, "Park's Vector Approach for Online Fault Diagnosis of Induction Motors", *IEEE International Conference on Information Communication and Embedded System,* pp. 1123-1129, 21-22 Feb. 2013, Chennai.

[34] Su Qianliet. al., "New Approach of Fault Detection and Fault Phase Selection Based on Initial Current Travelling Waves", *IEEE Power Energy Society Summer Meeting,* vol. 1, pp. 393-397, Conf. 25-25 July, 2002.

[35] M. Sifuzzamanet. al.,"Application of Wavelet Transform and its Advantages Compared to Fourier Transform", *Journal ofPhysical Sciences,* vol. 13, pp. 121-134, 2009

[36] E. Schmitt et. al., "Applications of Wavelets in Induction Machine Fault Detection"*Ingeniare.Revistachilena de ingeniería*, vol. 18, no. 2, pp. 158-164, 2010

[37] Tommy W. S. Chow and Shi Hai, "Induction Machine Fault Diagnostic Analysis with Wavelet Technique", *IEEE Transactions on Industrial Electronics,* vol. 51, no. 3, pp. 558-565, June 2004.

[38] PragasenPillayet. al., "A New Algorithm for Transient Motor Current Signature Analysis Using Wavelets", *IEEE Transactions on Industry Applications,* vol. 40, no. 5, pp. 1361-1368, Sept. /Oct. 2004.

[39] A.P. SakisMeliopoulos and Chien-Hsing Lee, "An Alternative Method for Transient Analysis via Wavelets", *IEEE Transactions on Power Delivery,* vol. 15, no. 1, pp. 114-121, January 2000.

[40] S.A. Salehet. al., "Application of a Wavelet-Based MRA for Diagnosing Disturbances in a Three-Phase Induction Motor", *5th IEEE International Symposium on Diagnostics for Electric Machines, Power Electronics and Drives,* pp. 1-6, 7-9 Sept. 2005, Vienna.

[41] M.A.S.K. Khan and M.A. Rahman, "Discrete Wavelet Transform Based Detection of Disturbances in Induction Motors", *4th International Conference on Electrical and Computer Engineering ICECE 2006,* pp. 462-465, *19-21* Dec. 2006, Dhaka, Bangladesh.

[42] Daniel T.L. Lee and Akio Yamamoto, "Wavelet Analysis: Theory and Applications", *Hewlett-Packard Journal,* pp. 44-52, Dec. 1994.

[43] Christopher Torrence and Gilbert P. Compo, "A Practical Guide to Wavelet Analysis", *Bulletin of the American Meterological Society,* vol. 79, no. 1, pp. 61-78, January 1998.

[44] KhalafSalloumGaeid and Hew Wooi Ping, "Wavelet fault diagnosis and tolerant of induction motor: A review", *International Journal of the Physical Sciences*, vol. 6(3), pp. 358-376, 4 February, 2011.

[45] Austin H. Bonnett and George C. Soukup, "Analysis of Rotor Failures in Squirrel-Cage Induction Motors", *IEEE Transactions on Industry Applications,* vol. 24, no. 6, pp. 1124-1130, Nov./Dec. 1988.

[46] G.B. Klimanet. al., "Non-invasive Detection of Broken Rotor Bars in Operating Induction Motors", *IEEE Transactions on Energy Conversion,* vol. 3, no. 4, pp. 873-879, Dec. 1988.

[47] Olivier Ondelet. al., "A Method to Detect Broken Bars in Induction Machine Using Pattern Recognition Techniques", *IEEE Transactions on Industry Applications,* vol. 42, no. 4, pp. 916-923, July/August 2006.

[48] A.J. Marques Cardoso, S.M.A. Cruz, J.F.S. Carvalho and E.S. Saraiva, "Rotor Cage Fault Diagnosis in Three-Phase Induction Motors, by Park's Vector Approach", *IEEE Industry Applications Conference,* vol. 1, pp. 642-646, 8-12 Oct. 1995, Oriando, FL.

[49] W. Deleroi, "Broken bars in squirrel cage rotor of an induction motor, Part 1: Description by superimposed fault currents", (in German), *Arch. f¨urElektrotechnik*, vol. 67, pp. 91–99, 1984.

[50] N. Benouzza, A. Benyettou, and A. Bendiabdellah, "An Advanced Park's Vector Approach For Rotor Cage Diagnosis", *IEEE First International Symposium on Control, Communications and Signal Processing,* pp. 461-464, 2004.

[51] ToomasVaimann, AnouarBelahcen, Javier Martinez, and AleksanderKilk, "Detection of Broken Bars in Frequency Converter Fed Induction Motor Using Park's Vector Approach", *IEEE Electric Power Quality and Supply Reliability Conference,* pp. 1-4, 11-13 June 2012, Tartu.

[52] HamidrezaBehbahanifrad, HamidrezaKarshenas, and AlirenzaSadoughi, "Non-Invasive On-line Detection of Winding Faults in Induction Motors- A Review", *IEEE International Conference on Condition Monitoring and Diagnosis,* Beijing, China, April 21-24, 2008.

[53] A. J. Marques Cardoso, S.M.A. Cruz and D.S.B. Fonseca, "Inter-Turn Stator Winding Fault Diagnosis in Three-Phase Induction Motors, by Park's Vector Approach", *IEEE Transactions on Energy Conversion,* vol. 14, no. 3, pp. 595-598, Sept. 1999.

[54] Austin H. Bonnett, "Cause and Analysis of Bearing Failures in Electrical Motors", *IEEE Industry Application Society 39th Annual Petroleum and Chemical Industry Conference,* pp. 87-95, 28-30 Sept. 1992, San Antonio, TX.

[55] Austin H. Bonnett, "Cause and Analysis of Anti-Friction Bearing Failures in A.C. Induction Motors", *IEEE Pulp and Paper Industry Technical Conference,* pp. 36-46, 21-25 June, 1993.

[56] José L. H. Silva and A. J. Marques Cardoso, "Bearing Failures Diagnosis in Three-Phase Induction Motors by Extended Park's Vector Approach", *31st Annual Conference of IEEE of Industrial Electronics Society,* 6-10 Nov. 2005.

[57] J. R. Cameron, W. T. Thomson, and A. B. Dow, "Vibration and Current Monitoring for Detecting Air-gap Eccentricity in Large Induction Motors", *Proceedings of Electrical Engineering,* vol. 133, pt. B, pp. 153-163, May 1986.

[58] J.F. Banguraet. al., "Diagnostics of Eccentricities and Bar/End-Ring Connector Breakages in Polyphase Induction Motors Through a Combination of Time-Series Data Mining and Time-Stepping Coupled FE-State-Space Techniques", *IEEE Transactions on Industry Applications,* vol. 39, no. 4, pp. 1005-1013, July/ August 2003.

[59] R.J. Povinelliet. al., "Diagnostics of Bar and End-Ring Connector Breakage Faults in Polyphase Induction Motors Through a Novel Dual Track of Time-Series Data Mining and Time-Stepping Coupled FE-State Space Modeling", *IEEE Transactions on Energy Conversion,* vol. 17, no. 1, pp. 39-46, March 2002.

[60] DamirŽarko, Drago Ban, Ivan Vazdar and Vladimir Jarić, "Calculation of Unbalanced Magnetic Pull in a Salient-Pole Synchronous Generator",*14th International Power Electronics and Motion Control Conference, EPE-PEMC,* pp. 116-122, 2010.

[61] Austin H. Bonnett, "Cause, Analysis and Prevention of Motor Shaft Failures", *IEEE Pulp and Paper Industry Technical Conference,* pp. 166-180, 21-26 June, 1998.

[62]R. Polikar, Wavelet Tutorial. [Online] , Available ; http: //.Rowan.edu/_polikar / WAVE

LETS/WTtutorial.html

[63] Shashi Raj Kapoor, NishantKhandelwal,ParikshitPareek, "Bearing fault analysis by signal energy calculation based signal processing technique in Squirrel Cage Induction Motor", *International Conference on Signal Propagation and Computer Technology,* pp. 33-38, July, 2014.